

See discussions, stats, and author profiles for this publication at: <https://www.researchgate.net/publication/231306241>

# Photooxidation of matrix-isolated iron pentacarbonyl. 1. Peroxo- and oxoiron carbonyl reaction intermediates

ARTICLE *in* INORGANIC CHEMISTRY · JUNE 1992

Impact Factor: 4.76 · DOI: 10.1021/ic00039a053

---

CITATIONS

23

---

READS

18

5 AUTHORS, INCLUDING:



**Anthony J Downs**

University of Oxford

258 PUBLICATIONS 5,009 CITATIONS

SEE PROFILE



**Matthew Almond**

University of Reading

122 PUBLICATIONS 1,260 CITATIONS

SEE PROFILE

Contribution from the Inorganic Chemistry Laboratory, University of Oxford, Oxford OX1 3QR, U.K., and Department of Chemistry, University of Reading, Reading RG6 2AD, U.K.

## Photooxidation of Matrix-Isolated Iron Pentacarbonyl. 1. Peroxo- and Oxoiron Carbonyl Reaction Intermediates

Michael Fanfarillo,<sup>1a,b</sup> Helen E. Cribb,<sup>1a</sup> Anthony J. Downs,<sup>\*1a</sup> Tim M. Greene,<sup>1a</sup> and Matthew J. Almond<sup>1c</sup>

Received November 27, 1991

The UV photolysis ( $\lambda = \text{ca. } 312 \text{ nm}$ ) of  $\text{Fe}(\text{CO})_5$  molecules isolated in  $\text{O}_2$ -doped Ar matrices at ca. 20 K has been monitored by reference to the IR spectra of the matrices. These spectra indicate that the photooxidation of  $\text{Fe}(\text{CO})_5$  proceeds, without any obvious signs of photoselectivity, via five distinct oxoiron carbonyl intermediates, A–E, with the release of CO and  $\text{CO}_2$ , ultimately to arrive at two binary iron oxide molecules, F and G. The identity and likely structure of each product have been deduced by analysis of the number, energies, and relative intensities of the IR absorptions, with particular reference to the response to  $^{13}\text{CO}$  and  $^{18}\text{O}$  enrichment. Hence the first detectable oxidation product A appears to be a peroxoiron derivative  $(\eta^2\text{-O}_2)\text{Fe}(\text{CO})_4$  in which the  $\text{O}_2$  ligand occupies a basal site in a square-pyramidal framework centered on iron and conforming to  $C_s$  symmetry. The coordinated  $\text{O}_2$  unit of A then suffers photodissociation, together with loss of CO, to afford B, which is dioxoiron tricarbonyl,  $\text{O}_2\text{Fe}(\text{CO})_3$ , incorporating a trigonal-pyramidal array of CO ligands only weakly bound to an  $\text{O}=\text{Fe}=\text{O}$  moiety with a bond angle near  $150^\circ$ . B undergoes thermal or photolytic ( $\lambda = \text{ca. } 312 \text{ nm}$ ) decay via two pathways. One results in further loss of CO to give C, which is believed to be dioxoiron monocarbonyl,  $\text{O}_2\text{FeCO}$ , and which may subsequently add a second molecule of  $\text{O}_2$  with the formation of E, tentatively identified as  $\text{O}_2\text{Fe}(\eta^2\text{-O}_2)\text{CO}$ . The other pathway results in elimination of  $\text{CO}_2$  to give D, which appears to be monooxiron monocarbonyl,  $\text{OFeCO}$ . A partial mechanism is proposed to accommodate the interrelationship existing between  $\text{Fe}(\text{CO})_5$  and these various oxoiron carbonyl derivatives A–E, and the results are compared and contrasted with the behaviors of related oxidation processes.

### 1. Introduction

Few chemical problems can have attracted more attention in recent years than the activation of dioxygen through coordination to a transition metal, with particular emphasis on systems where that transition metal is iron.<sup>2</sup> Central to such studies is the controlled transfer of oxygen to an organic molecule, a process of crucial importance not only in biology but also in the commercial production of numerous chemicals.<sup>2,3</sup> For example, activation of dioxygen opens up the prospect of a wide variety of reactions involving substrates ranging from hydrocarbons<sup>4a</sup> through alcohols<sup>4b</sup> to ketones,<sup>4c</sup> in processes mediated by transition-metal centers coordinated by ligands as varied as  $\text{O}^{2-}$ ,<sup>4a,c</sup>  $\text{R}^{4a,d}$  and  $\text{PR}_3$  ( $\text{R} = \text{organic group}$ ),<sup>4a,b,d</sup>  $\text{CO}$ ,<sup>4a,d</sup> and  $\text{C}_5\text{Me}_5$ .<sup>4c</sup> The most common (radical chain) pathway for oxygen transfer entails transition-metal-promoted autoxidation,<sup>3</sup> but more controlled oxidation may be achieved where the metal center and its ligand environment serve either as a template for the coordination of both substrate and  $\text{O}_2$  (as in cytochrome P-450)<sup>5</sup> or as the active oxidant (e.g.

Table I. Modes of Oxygen Binding in Iron Compounds<sup>8</sup>

	structure type	mode of ligation	naming	$\nu(\text{O}=\text{O})$ or $\nu(\text{Fe}=\text{O})$ ( $\text{cm}^{-1}$ )
I		$\eta^1\text{-O}_2$	superoxo	1030–1180
II		$\eta^2\text{-O}_2$	peroxo	750–950
III		$\eta^1:\eta^1\text{-O}_2$	$\mu$ -peroxo $\mu$ -superoxo	750–900 1050–1150
IV		$2 \times \eta^1\text{-O}$	dioxo	750–1000
V		$\eta^1\text{-O}$	monooxo	800–900

*tert*-butyl hydroperoxide in the epoxidation of allylic alcohol).<sup>6</sup> However, the details of the actual oxygen-transfer step in processes of this sort are still but poorly understood, and, although intermediates containing peroxide ligands have commonly been invoked,<sup>7a</sup> few such compounds have been isolated,<sup>7b</sup> and still fewer have been shown convincingly to bring about clean carbon–oxygen bond formation.<sup>7c</sup>

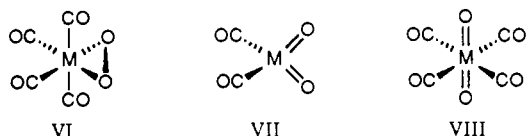
A primary objective must be an accurate description of the binding to the metal of dioxygen (and species derived from it) throughout the reaction sequence. Some of the modes by which oxygen binds to iron are listed in Table I.<sup>8</sup> The most prominent

- (1) (a) University of Oxford. (b) Present address: Pharmaceutical Department, ICI Pharmaceutical Division, Hurdfield Industrial Estate, Macclesfield, Cheshire SK10 2NA, U.K. (c) University of Reading.
- (2) *Molecular Mechanisms of Oxygen Activation*; Hayaishi, O., Ed.; Academic Press: New York, 1974. *Oxidases and Related Redox Systems*; King, T. E., Mason, H. S., Morrison, M., Eds.; Pergamon: Oxford, England, 1982. *Oxygen Complexes and Oxygen Activation by Transition Metals*; Martell, A. E., Sawyer, D. T., Eds.; Plenum Press: New York, 1988. *Metal Ion Activation of Dioxygen: Metal Ions in Biology*; Spiro, T. G., Ed.; Wiley-Interscience: New York, 1980; Vol. 2. Ingraham, L. L.; Meyer, D. L. *Biochemistry of Dioxygen (Biochemistry of the Elements, Vol. 4; Frieden, E., Series Ed.)*; Plenum Press: New York, 1985.
- (3) Sheldon, R. A.; Kochi, J. K. *Metal-Catalyzed Oxidations of Organic Compounds*; Academic Press: New York, 1981.
- (4) (a) Chambers, R. C.; Hill, C. L. *Inorg. Chem.* **1989**, *28*, 2509. Lee, J. S.; Oyama, S. T. *Catal. Rev. Sci. Eng.* **1988**, *30*, 249. Sheu, C.; Sawyer, D. T. *J. Am. Chem. Soc.* **1990**, *112*, 8212. Weber, L.; Haufe, G.; Rehorek, D.; Hennig, H. *J. Chem. Soc., Chem. Commun.* **1991**, 502. Kitajima, N.; Ito, M.; Fukui, H.; Moro-oka, Y. *J. Chem. Soc., Chem. Commun.* **1991**, 102. (b) Bilgrien, C.; Davis, S.; Drago, R. S. *J. Am. Chem. Soc.* **1987**, *109*, 3786. (c) Ali, B. E.; Brégeault, J.-M.; Mercier, J.; Martin, J.; Martin, C.; Convent O. *J. Chem. Soc., Chem. Commun.* **1989**, 825. (d) Lawson, H. J.; Atwood, J. D. *J. Am. Chem. Soc.* **1989**, *111*, 6223. (e) van Asselt, A.; Trimmer, M. S.; Henling, L. M.; Bercaw, J. E. *J. Am. Chem. Soc.* **1988**, *110*, 8254. Morse, D. B.; Rauchfuss, T. B.; Wilson, S. R. *J. Am. Chem. Soc.* **1988**, *110*, 8234. Parkin, G.; Bercaw, J. E. *J. Am. Chem. Soc.* **1989**, *111*, 391.
- (5) *Cytochrome P-450*; Sato, R., Omura, T., Eds.; Kodansha Ltd.: Tokyo, 1978. Guengerich, F. P.; Macdonald, T. L. *Acc. Chem. Res.* **1984**, *17*, 9.

- (6) Finn, M. G.; Sharpless, K. B. In *Asymmetric Synthesis*; Morrison, J. D., Ed.; Academic Press: New York, 1985; Vol. 5, p 247.
- (7) (a) Mimoun, H. In *Comprehensive Coordination Chemistry*; Wilkinson, G.; Gillard, R. D.; McCleverty, J. A., Eds.; Pergamon: Oxford, 1987; Vol. 6, p 317. (b) Faller, J. W.; Ma, Y. *Organometallics* **1988**, *7*, 559. Drouin, M.; Harrod, J. F. *Can. J. Chem.* **1985**, *63*, 353. Mason, M. G.; Ibers, J. A. *J. Am. Chem. Soc.* **1982**, *104*, 5153. van der Ent, A.; Onderdelinden, A. L. *Inorg. Chim. Acta* **1973**, *7*, 203. (c) van Asselt, A.; Santarsiero, B. D.; Bercaw, J. E. *J. Am. Chem. Soc.* **1986**, *108*, 8291.
- (8) Lever, A. B. P.; Gray, H. B. *Acc. Chem. Res.* **1978**, *11*, 348. Gubelman, M. H.; Williams, A. F. *Struct. Bonding (Berlin)* **1983**, *55*, 1. Valentine, J. S.; McCandlish, E. In *Electron Transport and Oxygen Utilization*; Ho, C., Ed.; Elsevier North Holland: Amsterdam, 1982; p 229. Greenwood, N. N.; Earnshaw, A. *Chemistry of the Elements*; Pergamon: Oxford, England, 1984; p 718. Nakamoto, K. *Infrared and Raman Spectra of Inorganic and Coordination Compounds*, 4th ed.; Wiley: New York, 1986.

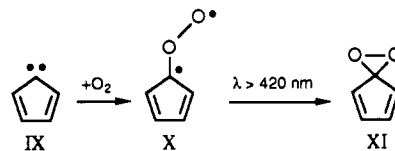
vibrational features, associated with the  $\nu(\text{O}=\text{O})$  or  $\nu(\text{Fe}=\text{O})$  fundamentals, occur at energies which provide a means of distinguishing between superoxo and other species but not between peroxy-, monooxo-, or dioxoiron derivatives. However, the response of the fundamental to  $^{18}\text{O}$  enrichment, particularly involving the unsymmetrical dioxygen isotopomer  $^{16}\text{O}^{18}\text{O}$ , is potentially a source of more definitive evidence regarding the mode of binding.<sup>9-13</sup>

One approach has exploited matrix-isolation methods to control and monitor the reaction between iron atoms and a simple oxygen-containing species, e.g.  $\text{O}$  and  $\text{O}_2$ <sup>14-16</sup> and ethylene oxide.<sup>17</sup> Hence, for example, the binary oxide molecules  $\text{FeO}$  and  $\text{FeO}_2$  have been identified, although the results affecting  $\text{FeO}_2$  are open to more than one interpretation,<sup>15,16</sup> and the presence of metal clusters, e.g.  $\text{Fe}_2$ , is an unavoidable complication. A strategy that mitigates the problem of products containing more than one metal atom entails UV photolysis of a metal carbonyl isolated at high dilution in an  $\text{O}_2$ -doped matrix. Experiments with  $\text{M}(\text{CO})_6$  molecules ( $\text{M} = \text{Cr}, \text{Mo},$  or  $\text{W}$ ) have revealed, for example, that photooxidation occurs in the presence of  $\text{O}_2$  giving oxometal carbonyl intermediates like VI, VII, and VIII<sup>10-12</sup> and, ultimately, binary metal oxides  $\text{MO}_x$  ( $x = 2, 3,$  or  $4$ ).<sup>13,18</sup> The coordinated  $\text{O}_2$  unit in the first detectable oxidation product  $(\eta^2\text{-O}_2)\text{M}(\text{CO})_4$ , VI, is activated with respect to photodissociation, such that irradiation at wavelengths near 360 nm (well above the threshold for photodissociation of free  $\text{O}_2$ <sup>19</sup>) causes rupture of the  $\text{O}-\text{O}$  bond and formation of dioxometal carbonyl derivatives like VII and VIII.



Here we turn our attention to the matrix photooxidation of iron pentacarbonyl. UV photolysis of this precursor gives rise in the first place to the 16-electron fragment  $\text{Fe}(\text{CO})_4$ <sup>20</sup> which may be expected to react with  $\text{O}_2$ . On the other hand,  $\text{Fe}(\text{CO})_4$  differs from  $\text{M}(\text{CO})_5$  ( $\text{M} = \text{Cr}, \text{Mo},$  or  $\text{W}$ ), the primary photoproduct of  $\text{M}(\text{CO})_6$ , in that it has not a singlet, but a triplet ground state,<sup>20,21</sup> and is likely therefore also to differ in its reactivity.<sup>22</sup> A further impetus to our research was provided by the results of recent matrix experiments concerning the interaction of  $\text{O}_2$  with various organic carbenes,<sup>23</sup> species bearing an isolobal relationship

to  $\text{Fe}(\text{CO})_4$ .<sup>24</sup> For example, cyclopentadienylidene IX combines thermally with  $\text{O}_2$  in an argon matrix to form the carbonyl oxide X, visible photolysis of which affords the corresponding dioxirane XI, representative of a class of molecules with unusual scope as oxygen transfer reagents.<sup>25</sup> Of particular note is the parallel between the oxidation products X and XI and the superoxo- (I) and peroxometal species (II) described above. In this paper we describe the results of our experiments in which the evolution of the matrix reactions has been charted by IR spectroscopy, the response to  $^{13}\text{CO}$ - and  $^{18}\text{O}$ -enrichment providing vital clues to the stoichiometries and likely structures of the products.



## 2. Experimental Section

The experiments were carried out broadly in accordance with the procedures described elsewhere.<sup>11-13,18</sup> An Air Products Displex CS 202 closed-cycle refrigerator gave window temperatures down to 17 K inside a shroud maintained at a pressure below  $10^{-7}$  Torr. Temperatures were measured with a chromel vs iron-doped gold thermocouple or with a hydrogen vapor bulb. Matrices were invariably formed by pulsed deposition.<sup>26</sup> IR spectra were recorded with a Perkin-Elmer Model 580A dispersive or a Mattson Galaxy FTIR spectrometer affording a resolution and accuracy not exceeding  $0.5\text{ cm}^{-1}$ . Calibration of the spectra recorded with the Model 580A was accomplished by superposition on the recorded spectrum of sharp vibrational/rotational or rotational lines due to gaseous  $\text{HCl}$ ,  $\text{DCl}$ ,  $\text{H}_2\text{O}$ ,  $\text{NH}_3$ , or  $\text{ND}_3$ .<sup>27</sup> UV-visible and Raman spectra were recorded on a Perkin-Elmer-Hitachi Model 330 and a Spex Ramalog 5 spectrophotometer, respectively.

Iron pentacarbonyl (ex Aldrich) was purified by fractional condensation in vacuo, the glass vacuum line being shrouded in aluminum foil to minimize the risk of photodecomposition. Samples of  $\text{Fe}(\text{CO})_5$  enriched in  $^{13}\text{CO}$  were prepared by photolysis of  $\text{Fe}(\text{CO})_5$  vapor (pressure ca. 0.1 Torr) in the presence of an excess of  $^{13}\text{CO}$  (99.3 atom %, Merck, Sharp and Dohme; 30 Torr) with the broad-band UV-visible emission from a 500-W medium-pressure mercury arc, typically over a period of 1 h.<sup>28,29</sup> The degree of enrichment was monitored by reference to the IR spectrum of the vapor. The resulting mixture was caused to bleed slowly through a spiral trap held at 77 K over a period of 5 h in order to separate efficiently the enriched sample of  $\text{Fe}(\text{CO})_5$  from the excess of  $\text{CO}$ . Argon and  $\text{O}_2$  were used as supplied by BOC (Research grade);  $^{18}\text{O}_2$  (98 atom %) was similarly used as supplied by Merck, Sharp and Dohme. In order to prepare a mixture of the isotopomers  $^{16}\text{O}_2$ ,  $^{16}\text{O}^{18}\text{O}$ , and  $^{18}\text{O}_2$ , a gas mixture of  $^{16}\text{O}_2$  and  $^{18}\text{O}_2$  in equimolar proportions was subjected to the action of an electrical discharge (excited by a Tesla coil) and the ozone thus generated trapped in a cold finger at 77 K. After the discharge had been halted, the ozone was allowed to vaporize so that it could be decomposed by broad-band UV-visible irradiation (via a quartz window). This procedure was repeated 8 or 9 times using relatively brief discharge and photolysis times (about 30 min). Any residual ozone remaining in the mixture was scavenged by exposure to clean mercury contained in a side-arm of the apparatus. The composition of the resulting mixture of  $^{16}\text{O}_2$ ,  $^{16}\text{O}^{18}\text{O}$ , and  $^{18}\text{O}_2$  was assessed by reference to the Raman spectrum of a sample isolated in an Ar matrix.

There was a choice of photolysis sources, namely a Philips HPK 125-W or an Oriel 500-W medium-pressure mercury arc. A 40-mm column of water contained in a quartz cell was used to minimize the intensity of IR radiation incident upon a given matrix during photolysis. In addition, the following filters were used, where appropriate: (a) a Balzers' interference filter transmitting radiation near 312 nm; (b) a  $\text{Cl}_2$  gas absorption filter transmitting radiation in the ranges  $220 < \lambda < 280$  and  $\lambda > 450$  nm; (c) a  $\text{Br}_2$  vapor absorption filter transmitting radiation in the ranges  $290 < \lambda < 370$  and  $\lambda > 550$  nm.<sup>30</sup> In order to overcome

- (9) Loehr, T. M. In *Oxygen Complexes and Oxygen Activation by Transition Metals*; Martell, A. E.; Sawyer, D. T., Eds.; Plenum Press: New York, 1988; p 17.
- (10) Poliakoff, M.; Smith, K. P.; Turner, J. J.; Wilkinson, A. J. *J. Chem. Soc., Dalton Trans.* **1982**, 651.
- (11) Crayston, J. A.; Almond, M. J.; Downs, A. J.; Poliakoff, M.; Turner, J. J. *Inorg. Chem.* **1984**, 23, 3051.
- (12) Almond, M. J.; Crayston, J. A.; Downs, A. J.; Poliakoff, M.; Turner, J. J. *Inorg. Chem.* **1986**, 25, 19.
- (13) Almond, M. J.; Downs, A. J. *J. Chem. Soc., Dalton Trans.* **1988**, 809.
- (14) Green, D. W.; Reedy, G. T.; Kay, J. G. *J. Mol. Spectrosc.* **1979**, 78, 257.
- (15) Abramowitz, S.; Acquisti, N.; Levin, I. W. *Chem. Phys. Lett.* **1977**, 50, 423.
- (16) Chang, S.; Blyholder, G.; Fernandez, J. *Inorg. Chem.* **1981**, 20, 2813.
- (17) Kafafi, Z. H.; Hauge, R. H.; Billups, W. E.; Margrave, J. L. *J. Am. Chem. Soc.* **1987**, 109, 4775.
- (18) Almond, M. J.; Hahne, M. J. *J. Chem. Soc., Dalton Trans.* **1988**, 2255.
- (19) Lin, C.-L.; DeMore, W. B. *J. Phys. Chem.* **1973**, 77, 863.
- (20) Poliakoff, M.; Turner, J. J. *J. Chem. Soc., Dalton Trans.* **1974**, 2276.
- (21) Poliakoff, M. *Chem. Soc. Rev.* **1978**, 7, 527. Poliakoff, M.; Weitz, E. *Acc. Chem. Res.* **1987**, 20, 408.
- (22) Barton, T. J.; Grinter, R.; Thomson, A. J.; Davies, B.; Poliakoff, M. *J. Chem. Soc., Chem. Commun.* **1977**, 841. Burdett, J. K. *J. Chem. Soc., Faraday Trans. 2* **1974**, 70, 1599. Elian, M.; Hoffmann, R. *Inorg. Chem.* **1975**, 14, 1058.
- (23) Seder, T. A.; Church, S. P.; Ouderkirk, A. J.; Weitz, E. *J. Am. Chem. Soc.* **1985**, 107, 1432.
- (24) Bell, G. A.; Dunkin, I. R. *J. Chem. Soc., Chem. Commun.* **1983**, 1213. Dunkin, I. R.; Shields, C. J. *J. Chem. Soc., Chem. Commun.* **1986**, 154. Bell, G. A.; Dunkin, I. R.; Shields, C. J. *Spectrochim. Acta, Part A* **1985**, 41A, 1221. Chapman, O. L.; Hess, T. C. *J. Am. Chem. Soc.* **1984**, 106, 1842.

- (24) Hoffmann, R. *Angew. Chem., Int. Ed. Engl.* **1982**, 21, 711.
- (25) Adam, W.; Curci, R.; Edwards, J. O. *Acc. Chem. Res.* **1989**, 22, 205.
- (26) Perutz, R. N.; Turner, J. J. *J. Chem. Soc., Faraday Trans. 2* **1973**, 69, 452.
- (27) *Tables of Wavenumbers for the Calibration of Infrared Spectrometers*, 2nd ed.; IUPAC Commission on Molecular Structure and Spectroscopy; Cole, A. R. H., compiler; Pergamon: Oxford, England, 1977.
- (28) Crichton, O.; Rest, A. J. *Inorg. Nucl. Chem. Lett.* **1973**, 9, 391.
- (29) Perutz, R. N.; Turner, J. J. *Inorg. Chem.* **1975**, 14, 262. Perutz, R. N. Ph.D. Thesis, University of Cambridge, 1974.

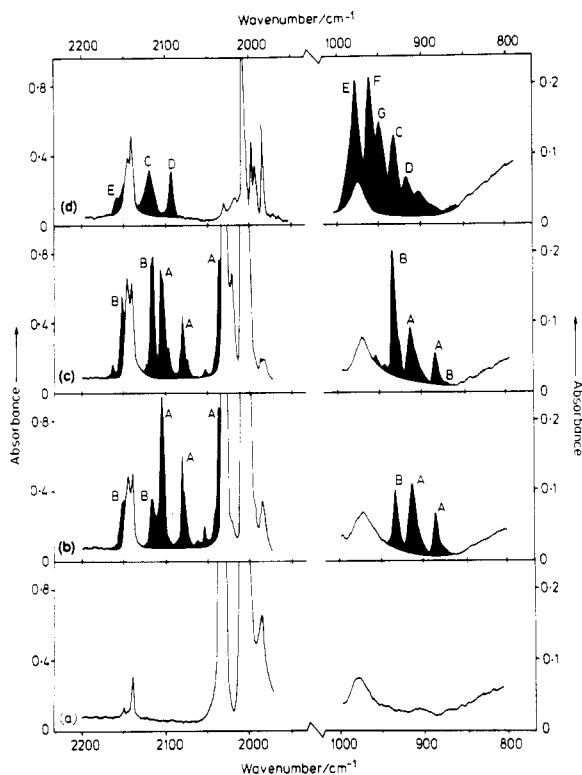


**Figure 1.** IR spectrum of  $\text{Fe}(\text{CO})_5$  isolated in an  $\text{O}_2$ -doped Ar matrix ( $\text{Ar}:\text{O}_2:\text{Fe}(\text{CO})_5 = \text{ca. } 1000:50:1$ ) in the regions 1950–2200 and 800–1000  $\text{cm}^{-1}$  showing the effects of photolysis at wavelengths near 312 nm: (a) after deposition, (b) after 60 min of photolysis, (c) after 160 min of photolysis, and (d) after 360 min of photolysis at  $\lambda = \text{ca. } 312$  nm followed by a further 200 min of photolysis using a  $\text{Br}_2$  filter ( $290 \leq \lambda \leq 370$  and  $\lambda \geq 550$  nm). Bands with black infilling are due to the products A–G. The broad band centered near 970  $\text{cm}^{-1}$  in these and other spectra is associated with an impurity on or in the CsI window.

the unusual photosensitivity of  $\text{Fe}(\text{CO})_4$ ,<sup>20</sup> a germanium filter 50 mm in diameter and 5 mm thick (Oriel) was used to intercept the radiation from the IR spectrometer source before it reached the matrix.

The wavenumbers and relative intensities of the  $\nu(\text{CO})$  features in the IR spectra of individual products incorporating  $\text{Fe}(\text{CO})_x$  fragments at varying levels of  $^{13}\text{CO}$  enrichment were calculated on the basis of an energy-factored force field using simple iterative refinement programs; IR spectra were then simulated with a program that constructed Lorentzian band shapes based on the calculated intensities.<sup>29,31</sup> The calculations were performed on a VAX computer operated by the Oxford University Computing Service.

### 3. Results and Discussion

**3.1. Overview.** An argon matrix containing  $\text{Fe}(\text{CO})_5$  and  $\text{O}_2$ , typically in the proportions  $\text{Ar}:\text{O}_2:\text{Fe}(\text{CO})_5 = 1000:50:1$  and held at 20 K, was irradiated with UV light at wavelengths close to 312 nm. At regular intervals the IR spectrum of the matrix was recorded. In addition to absorptions arising from  $\text{Fe}(\text{CO})_4$ ,<sup>20</sup> free  $\text{CO}$ ,<sup>32</sup> and free  $\text{CO}_2$ ,<sup>33</sup> several other new features developed with photolysis, these occurring, as illustrated in Figure 1, in the regions of the IR spectrum associated with  $\nu(\text{C}=\text{O})$  (1700–2200  $\text{cm}^{-1}$ ) and either  $\nu(\text{M}=\text{O})$  or  $\nu(\text{O}=\text{O})$  fundamentals (700–1100  $\text{cm}^{-1}$ ). The new bands formed in the earlier stages can be identified with intermediate oxoiron carbonyl molecules containing both CO and oxygen coordinated to the iron atom; each intermediate could be distinguished by the rate of growth and subsequent decay expe-

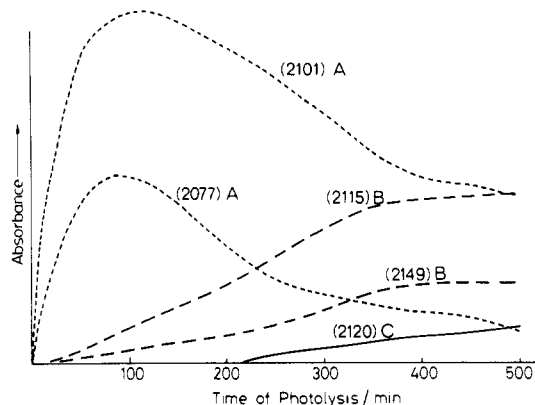


**Figure 2.** Plots showing changes in the intensities of selected IR bands associated with the photoproducts A, B, and C as a function of photolysis time. Numbers in parentheses give the wavenumbers ( $\text{cm}^{-1}$ ) of the relevant bands.

**Table II.** IR Absorptions Characteristic of the Matrix Photoproducts A–G

photoproduct	wavenumber ( $\text{cm}^{-1}$ )	
	$\nu(\text{C}=\text{O})^a$	$\nu(\text{O}=\text{O})$ or $\nu(\text{Fe}=\text{O})^a$
A	ca. 2140 vw <sup>b</sup>	914 w
	2101 s	885 w
	2077 m	
	2032 s	
B	2149 m	934 w
	2115 m	851 vw
C	2120 m	929 w
		874 vw
D	2095 m	920 w
E	2155 vw	970 w
F	–	956 w
G	–	945 w

<sup>a</sup> Error limits  $\pm 2$   $\text{cm}^{-1}$ . Key: s, strong; m, medium; w, weak; v, very.

<sup>b</sup> Not definitely observed; obscured by bands due to free  $^{12}\text{CO}$ .

rienced by its IR bands on continued UV photolysis. The final stages of prolonged photolysis (typically after a period of more than 3 h) witnessed the appearance and growth of yet more IR bands, now confined to the region 800–1000  $\text{cm}^{-1}$  and which could be identified with the formation of binary iron oxide molecules, representing the ultimate metal-containing photooxidation products.

By monitoring the growth and decay patterns of the bands, it is possible to assign each of them to one of *five* oxoiron carbonyl intermediates (A to E) or to one of *two* binary iron oxides (F and G). For example, Figure 2 shows clearly the growth and decay patterns characteristic of the bands assigned to intermediates A, B, and C. Table II lists all the spectroscopic features observed for the photoproducts A–G. Annealing the matrices at temperatures up to 33 K, following irradiation, was observed to have little effect on the bands due to the intermediate A but, in the later stages of photolysis, to favor the accretion of the species C–G at the expense of B. In this paper we are concerned with the identification and characterization of the oxoiron carbonyl intermediates A–E. The iron oxide molecules F and G will be treated in a separate paper.<sup>34</sup>

As Figure 1 will testify, the existence of seven different iron-containing oxo products, together with free CO and  $\text{CO}_2$ ,  $\text{Fe}(\text{CO})_4$ , and unchanged  $\text{Fe}(\text{CO})_5$ , resulted in IR spectra that were relatively congested with absorptions in the regions 1900–2400  $\text{cm}^{-1}$  and 800–1000  $\text{cm}^{-1}$ . It was inevitable in the circumstances that the absorptions of certain matrix components should overlap, causing some features to be partially or wholly obscured. Not only did this mean that some information was liable to be lost without trace, there were also considerable problems with assessing the *relative*

(30) Rest, A. J.; Sodeau, J. R.; Taylor, D. J. *J. Chem. Soc., Dalton Trans.* **1978**, 651.

(31) Church, S. P.; Poliakoff, M.; Timney, J. A.; Turner, J. J. *Inorg. Chem.* **1983**, 22, 3259. In fact, the dimensions given for model XVI are not strictly possible but close to the values of 96.5 and 160° which are both physically acceptable and consistent with the observed  $\nu(\text{C}=\text{O})$  spectra.

(32) Dubost, H. *Chem. Phys.* **1976**, 12, 139.

(33) Fredin, L.; Nelander, B.; Ribbegård, G. *J. Mol. Spectrosc.* **1974**, 53, 410. Guasti, R.; Schettino, V.; Brigot, N. *Chem. Phys.* **1978**, 34, 391.

(34) Part 2: Fanfarillo, M.; Downs, A. J.; Greene, T. M.; Almond, M. J. *Inorg. Chem.*, following paper in this issue.

intensities of some of the bands which could be identified with a particular absorber. Thus, although two of the  $\nu(\text{C}=\text{O})$  bands believed to originate in the intermediate A fell in regions that were otherwise more-or-less transparent, a third, occurring near 2032  $\text{cm}^{-1}$ , could be discerned only as a shoulder on the high-energy flank of an intense band originating in unchanged  $\text{Fe}(\text{CO})_5$ . As a result we could gauge only roughly the intensity of the third band, relative to the other two. A similar, but less acute, problem was presented by one of the two  $\nu(\text{C}=\text{O})$  bands we attribute to B and which, with an energy of 2149  $\text{cm}^{-1}$ , was partially overlaid by the absorptions due to free CO in one form or another.<sup>32</sup> Such complications were exacerbated of course when steps were taken to examine the effects of  $^{13}\text{CO}$  or  $^{18}\text{O}$  enrichment (*quod vide*). As in other matrix studies involving the photolysis of a metal carbonyl in the presence of a potential reagent,<sup>11-13,18,29,31,35,36</sup> precursor and product bands were invariably rather broad, with fwhm's sometimes exceeding 5  $\text{cm}^{-1}$ , and frequently betrayed evidence of splitting. This property, which we take to be a function of the different matrix sites accessible to a particular guest, limited the definition which we were able to achieve in our IR detection; more seriously it complicated the interpretation of the photochemical changes. Thus, not only did the occupancy of different sites by the parent  $\text{Fe}(\text{CO})_5$  molecule lead to splitting of the vibrational transitions but it also discriminated between the molecules as regards their photolability. Photolysis resulted therefore in changes in the intensity patterns of the wholly or partially resolved multiplets due to the  $\text{Fe}(\text{CO})_5$  molecule, as noted previously,<sup>37</sup> and so foiled attempts at spectral subtraction. A similar problem with the matrix photolysis of  $\text{HMn}(\text{CO})_5$  has been successfully countered by the stratagem of "reverse" photolysis.<sup>31</sup> Unfortunately, however, this solution could not be applied to the photooxidation of  $\text{Fe}(\text{CO})_5$ , for the reasons now to be explained.

In contrast to the behavior of other systems involving metal carbonyls, the photooxidation of  $\text{Fe}(\text{CO})_5$  appeared to be marked by a relatively indiscriminate response to the wavelength of the photolyzing radiation. In the matrix photooxidation of the group 6 hexacarbonyls  $\text{M}(\text{CO})_6$  ( $\text{M} = \text{Cr}, \text{Mo}, \text{or } \text{W}$ ), it was found that irradiating the matrix with light of different wavelengths causes the selective buildup of specific intermediates.<sup>11,12</sup> The  $\text{Fe}(\text{CO})_5/\text{O}_2$  system exhibited little or no such selectivity and no sign of reversibility, so far as we could detect. Thus, in order to build up significant concentrations of A, B, or C, we were obliged to irradiate the matrix with light having wavelengths near 312 nm for a period of time carefully chosen so as to optimize the yield of a particular intermediate (see Figure 2). This approach meant, however, that it was impossible to generate a high yield of C without having simultaneously a relatively high concentration of B in the matrix. Moreover, intermediates D and E were invariably produced only in very low yields. We found that the maximum possible concentrations of these species were realized after irradiation of the matrix first at  $\lambda = \text{ca. } 312 \text{ nm}$  for 200–500 min and then at  $\lambda = 290\text{--}370 \text{ nm}$  for 40–200 min.

This lack of photoselectivity was also conspicuous in supplementary experiments carried out to measure the UV-visible absorption spectrum of a methane matrix containing  $\text{Fe}(\text{CO})_5$  and  $\text{O}_2$  with the composition  $\text{CH}_4:\text{O}_2:\text{Fe}(\text{CO})_5 = \text{ca. } 1000:50:1$ . Irradiation of the matrix at wavelengths near 312 nm gave no sign of the bands characteristic of  $\text{Fe}(\text{CO})_4$ ,<sup>20</sup> nor was it possible to discern clearly the growth of any new individual absorptions. However, the use of subtraction routines did bring to light the growth of distinct UV absorptions at wavelengths shorter than 350 nm; centered at  $\lambda_{\text{max}} = 210, 260, \text{ and } 320 \text{ nm}$ , these are probably associated with one or both of the intermediates A and B. Prolonged UV photolysis (for a total of ca. 4 h) failed to reveal any other features, the results of subtraction routines becoming increasingly unreliable as the optical properties of the matrix

deteriorated and the sample became depleted in strongly absorbing species.

Attempts to monitor the progress of the photooxidation by reference to the Raman spectrum of a methane matrix containing  $\text{Fe}(\text{CO})_5$  and  $\text{O}_2$  (excited at  $\lambda = 647.1 \text{ nm}$ ) met with very limited success. The spectrum recorded rapidly after a short period of UV photolysis did show evidence of new scattering attributable to the oxometal carbonyl species A, B, and C, as well as free CO. It was impossible, however, to detect any new bands in the region associated with  $\nu(\text{Fe}=\text{O})$  or  $\nu(\text{O}=\text{O})$  modes, and the photolability of the oxometal carbonyls with respect to the high flux of the probe radiation (even at  $\lambda = 647.1 \text{ nm}$ ) militated against readily reproducible results. Hence further studies along these lines did not seem to be warranted.

The production of free  $\text{CO}$ <sup>32</sup> and free  $\text{CO}_2$ <sup>33</sup> was a feature of all the IR experiments in which matrix-isolated  $\text{Fe}(\text{CO})_5$  was photolyzed in the presence of dioxygen. Two significant aspects caught our attention. In the first place, the bands associated with  $\text{CO}_2$  appeared and grew *only* in the stages following the decay of photoproduct B. This suggests that B may undergo photodecomposition by loss of  $\text{CO}_2$ . In the second place, we observed that virtually all the CO photoejected from  $\text{Fe}(\text{CO})_5$  and its photoproducts was oxidized ultimately to  $\text{CO}_2$ . On the evidence of our experiments, moreover, it appeared that only CO molecules trapped within the matrix cage, and therefore coordinated—if only loosely—to the iron metal center, were so oxidized. This point was reinforced by a control experiment in which a 5%  $\text{O}_2$ -doped argon matrix containing CO, *but no*  $\text{Fe}(\text{CO})_5$ , was photolyzed with radiation having  $\lambda = \text{ca. } 312 \text{ nm}$ . This resulted, even after photolysis over 24 h, in a very low yield of  $\text{CO}_2$ , 1–2 orders of magnitude smaller than that achieved in similar circumstances through the photooxidation of  $\text{Fe}(\text{CO})_5$ .

We have investigated the effects of varying the matrix concentration of  $\text{Fe}(\text{CO})_5$  (from 0.1 to 0.02%) and of  $\text{O}_2$  (from 1 to 10%). Reducing the concentration of  $\text{Fe}(\text{CO})_5$  caused merely a uniform reduction in the intensities of all the IR bands associated with the different photoproducts. The growth of the IR absorptions due to intermediates A to D does not depend significantly on the  $\text{O}_2$  concentration, but the absorptions due to the photoproducts E to G grew substantially more slowly at low  $\text{O}_2$  concentrations. This suggests that two or more  $\text{O}_2$  molecules are involved, at one stage or another, in the photolytically induced reactions affording E, F, and G. Some experiments carried out with pure  $\text{O}_2$  matrices gave results similar to those involving  $\text{O}_2$ -rich argon matrices, but at the expense of still broader product bands and with little advantage to the concentrations of the products (a finding attributable, presumably, to the inferior optical properties of the deposits).

Our strategy for identifying the intermediates A to E was as follows. Firstly, we compared the number, energies, and relative intensities of the  $\nu(\text{C}=\text{O})$  absorptions attributable to each intermediate with the features expected for an  $\text{Fe}(\text{CO})_x$  fragment subject to variations of stoichiometry and geometry. Secondly, we carried out experiments leading to partial enrichment of the intermediate in  $^{13}\text{CO}$ . These entailed matrix photooxidation of  $\text{Fe}(^{12}\text{CO})_{5-n}(^{13}\text{CO})_n$  isotopomers (where  $n = 0$  to 5) with overall levels of  $^{13}\text{CO}$  enrichment amounting to 25, 50, or 83%. With the additional information thus derived, we were able once again to compare the number, energies, and relative intensities of the observed  $\nu(\text{C}=\text{O})$  bands with the patterns calculated for different  $\text{Fe}(\text{CO})_x$  fragments.<sup>29,31,38,39</sup> Via intensity measurements it is also possible, at least in some cases, to estimate the OC–Fe–CO bond angles of the  $\text{Fe}(\text{CO})_x$  fragments.<sup>39</sup>

The mode of coordination of the oxygen to the iron center we determined by reference to the effects of  $^{18}\text{O}$  enrichment. Two types of experiment were performed, one utilizing a mixture of

(35) Horton-Mastin, A.; Poliakoff, M.; Turner, J. J. *Organometallics* **1986**, 5, 405. See also McHugh, T. M.; Rest, A. J. *J. Chem. Soc., Dalton Trans.* **1980**, 2323.

(36) McHugh, T. M.; Rest, A. J.; Taylor, D. J. *J. Chem. Soc., Dalton Trans.* **1980**, 1803.

(37) Poliakoff, M.; Turner, J. J. *J. Chem. Soc., Dalton Trans.* **1973**, 1351.

(38) (a) Darling, J. H.; Ogden, J. S. *J. Chem. Soc., Dalton Trans.* **1972**, 2496; **1973**, 1079. (b) Burdett, J. K. *Coord. Chem. Rev.* **1978**, 27, 1; *Inorg. Chem.* **1981**, 20, 2607.

(39) Burdett, J. K.; Poliakoff, M.; Turner, J. J.; Dubost, H. *Adv. Infrared Raman Spectrosc.* **1976**, 2, 1.

**Table III.** Wavenumbers ( $\text{cm}^{-1}$ ) of IR Bands Due to  $\nu(\text{C-O})$  Modes of  $\text{Fe}(\text{CO})_5$  Isolated in an Ar Matrix before and after Short Periods of UV Photolysis in the Presence of  $\text{O}_2^a$ 

Fe(CO) <sub>5</sub> alone in Ar matrix		Fe(CO) <sub>5</sub> in 5% O <sub>2</sub> -doped Ar matrix				assignment
on deposition	after photolysis <sup>b</sup>	on deposition <sup>c</sup>	after photolysis <sup>b</sup>	effect of photolysis for 20 min <sup>b,c</sup>	effect of photolysis for 40 min <sup>b,c</sup>	
	2140.4		2149.6	app	↑	CO + A? <sup>d</sup> + B
			2143.3	app		
			2113.9		app	
			2102.8	app	↑	B
			2100.9	app	↑	
			2099.7	app	↑	A <sup>d</sup>
			2078.2	app	↑	
			2075.6	app	↑	A <sup>d</sup>
2034.1	2033.9	2034.1	2033.9	↑	↑	
			2030.3	app	↑	Fe(CO) <sub>5</sub> (a <sub>2</sub> '') <sup>e</sup> + A <sup>d</sup>
			2024.7		↑	
2025.0	2024.7	2025.7			↑	Fe(CO) <sub>5</sub> (a <sub>2</sub> '') <sup>e</sup>
2023.0	2022.8	2024.0 (sh)		↓	↑	
2007.8	2007.8	2007.4	2007.6	↓	↑	Fe(CO) <sub>5</sub> (e') <sup>e</sup>
2005.2	2005.2	2004.6	2004.5	↓	↑	
2003.0	2003.0	2002.5	2002.8	↓	↑	
1997.7	1997.5	1998.2	1997.7	↓	↑	
	1996.5				↑	Fe(CO) <sub>4</sub> (a <sub>1</sub> ) <sup>e</sup>
	1995.3		1995.1	app	↑	
	1991.2		1991.2	app	↑	Fe(CO) <sub>4</sub> (b <sub>1</sub> ) <sup>e</sup>
	1988.8		1989.0	app	↑	
	1972.6		1972.6	app	↑	Fe(CO) <sub>4</sub> (b <sub>2</sub> ) <sup>e</sup>
	1970.5		1971.0	app	↑	
	1968.3		1968.5	app	↑	Fe(CO) <sub>3</sub> (e) <sup>e</sup>
	1932.4				↑	

<sup>a</sup> Dilution Ar:Fe(CO)<sub>5</sub> = ca. 2000:1. <sup>b</sup>  $\lambda$  = ca. 312 nm. <sup>c</sup> Key: sh, shoulder; app, band appears; ↑, band grows; ↓, band decays. <sup>d</sup> Estimated band centers for A: ca. 2140, 2101.1, 2076.9, and 2032.1  $\text{cm}^{-1}$  (see Table II). <sup>e</sup> See ref 20.

the two "symmetrical" isotopomers  $^{16}\text{O}_2$  and  $^{18}\text{O}_2$ , the other utilizing a scrambled mixture of all the isotopomers  $^{16}\text{O}_2$ ,  $^{16}\text{O}^{18}\text{O}$ , and  $^{18}\text{O}_2$ . The first type of experiment allows us to measure the  $^{16}\text{O}$ - $^{18}\text{O}$  isotopic shift and to assess whether addition of  $\text{O}_2$  proceeds by a concerted or nonconcerted mechanism. The second allows us to distinguish a monooxoiron fragment,  $\text{FeO}$  (V), from a fragment of the type  $\text{FeO}_2$  with the possible structures I, II, or IV (see Table I). The  $\nu(\text{Fe}=\text{O})$  feature of V is expected to give rise to a doublet, whereas each  $\nu(\text{Fe}=\text{O})$  or  $\nu(\text{O}-\text{O})$  mode of I, II, or IV is most likely to give rise to a triplet pattern, with components identifiable with the isotopomers  $\text{Fe}^{16}\text{O}_2$ ,  $\text{Fe}^{16}\text{O}^{18}\text{O}$ , and  $\text{Fe}^{18}\text{O}_2$ , respectively.<sup>10-13,40</sup> The energy of the central feature resulting from the  $\text{Fe}^{16}\text{O}^{18}\text{O}$  molecule is then of crucial importance in distinguishing between the structures I, II, and IV. If this feature is *unsymmetrically* disposed between the two outer features, the absorption is likely to arise from a  $\nu(\text{Fe}=\text{O})$  fundamental of a dioxoiron unit (IV),<sup>10-13,41</sup> whereas a *symmetrical* pattern of bands points to a  $\nu(\text{O}-\text{O})$  fundamental of a coordinated dioxygen molecule (I or II).<sup>12</sup>

In the event of a fragment with the structure IV, the  $\text{O}=\text{Fe}=\text{O}$  bond angle may be estimated either from the relative intensities of the absorptions due to the antisymmetric and symmetric  $\nu(\text{Fe}=\text{O})$  modes<sup>42</sup> or from the  $^{16}\text{O}$ - $^{18}\text{O}$  shift displayed by one or both of these modes (the antisymmetric  $\nu(\text{Fe}=\text{O})$  mode is often the only one to be observed).<sup>11,12,41,43</sup> The second method gives rise strictly to an *upper* limit to the bond angle, at least in the absence of information about the anharmonicity corrections.<sup>43</sup>

On this basis we have been able to identify more-or-less certainly the five intermediate molecules A to E which are generated by photooxidation of  $\text{Fe}(\text{CO})_5$  in  $\text{O}_2$ -doped argon matrices at 20 K.

**3.2. Intermediate A. (a)  $\nu(\text{C-O})$  Region.** Intermediate A is characterized by at least three IR bands in the spectral region

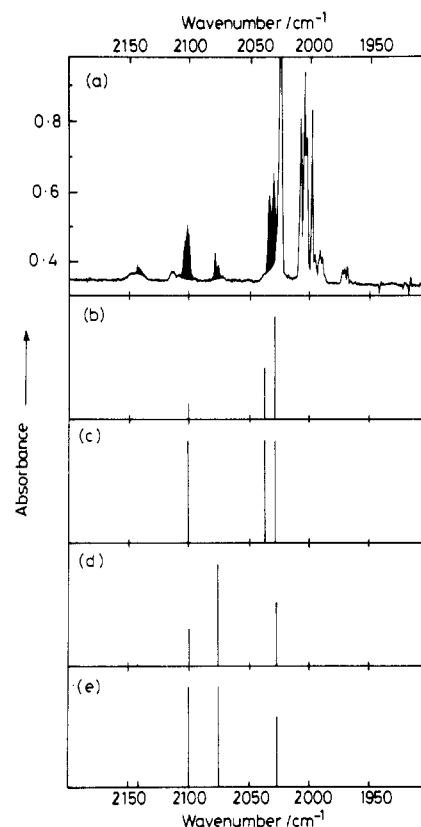


**Figure 3.** Comparison of (a) the IR spectrum observed for A in the  $\nu(\text{C-O})$  region (Ar:O<sub>2</sub>:Fe(CO)<sub>5</sub> = ca. 2000:100:1; photolysis for 40 min at  $\lambda$  = ca. 312 nm; bands due to A distinguished by black infilling) with schematic representations of the corresponding spectra characteristic of the following units: (b)  $\text{Fe}(\text{CO})_3$  with  $C_{2v}$  symmetry (model XII); (c)  $\text{Fe}(\text{CO})_3$  with  $C_s$  symmetry (model XIII); (d)  $\text{Fe}(\text{CO})_4$  with  $C_{2v}$  symmetry (model XIV); and (e)  $\text{Fe}(\text{CO})_4$  with  $C_s$  symmetry (model XV).

associated with C-O stretching fundamentals, these being centered at 2032, 2077, and 2101  $\text{cm}^{-1}$  (see Tables II and III). There is also the possibility of a fourth, weak band near 2140  $\text{cm}^{-1}$ , but

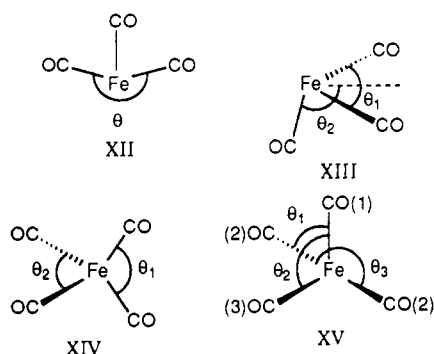
(40) In principle, I can be distinguished from II by the observation of not one but two features associated with the  $\nu(\text{O}-\text{O})$  mode of the  $\text{M}^{16}\text{O}^{18}\text{O}$  isotopomer; in practice, such a pattern is seldom observed, even for authentic superoxometal derivatives. See, for example, Darling, J. H.; Garton-Sprenger, M. B.; Ogden, J. S. *Faraday Symp. Chem. Soc.* **1973**, 8, 75.

(41) See, for example, Green, D. W.; Ervin, K. M. *J. Mol. Spectrosc.* **1981**, 89, 145.

(42) See, for example, Smit, W. M. A. *J. Mol. Struct.* **1973**, 19, 789.

(43) Green, D. W.; Ervin, K. M. *J. Mol. Spectrosc.* **1981**, 88, 51.

the absorptions hereabouts due to free CO,<sup>32</sup> which grew at the same rate as those due to A, made it impossible to confirm the authenticity of this feature. These observations suggest that A contains an Fe(CO)<sub>3</sub> or Fe(CO)<sub>4</sub> fragment of relatively low symmetry (the presence of more than four CO groups is ruled out by the observation that A is formed from Fe(CO)<sub>5</sub> with the elimination of free CO). Figure 3 compares the spectrum associated with A with schematic representations of the patterns typifying the following units: (i) an Fe(CO)<sub>3</sub> unit with C<sub>2v</sub> symmetry (XII), as in (η<sup>2</sup>-alkene)<sub>2</sub>Fe(CO)<sub>3</sub>;<sup>44</sup> (ii) an Fe(CO)<sub>3</sub> unit with C<sub>s</sub> symmetry (XIII), as in (η<sup>4</sup>-diene)Fe(CO)<sub>3</sub>;<sup>45</sup> (iii) an Fe(CO)<sub>4</sub> unit with C<sub>2v</sub> symmetry (XIV), as in free Fe(CO)<sub>4</sub>;<sup>20</sup> (iv) an Fe(CO)<sub>4</sub> unit with C<sub>s</sub> symmetry (XV) akin to the Mn(CO)<sub>4</sub> fragment in the C<sub>s</sub> isomer of HMn(CO)<sub>4</sub>.<sup>31</sup> Allowance must be made for the fact that an Fe(CO)<sub>4</sub> unit with C<sub>2v</sub> or C<sub>s</sub> symmetry allows considerable variation in the precise wavenumber and intensity patterns for the three modes at lower energy, the essential feature being that these are of comparable intensity and at least an order of magnitude more intense than the high-energy mode. Hence it appears that the observed spectrum is more compatible with an Fe(CO)<sub>4</sub> unit (model XIV or XV) than with an Fe(CO)<sub>3</sub> unit (model XII or XIII). On the other hand, calculations employing a range of bond angles and force constants show that the observed spectrum can be reproduced more or less closely by any one of the four models if sufficient latitude is admitted to the choice of geometry and force constants (albeit at some cost to plausibility in certain cases, e.g. model XII for which the angle θ is required to be 110°). Therefore, although Fe(CO)<sub>4</sub> seems on balance more likely than Fe(CO)<sub>3</sub>, we cannot on the basis of this information alone infer definitely either the stoichiometry or the geometry adopted by the Fe(CO)<sub>x</sub> fragment.



In order to resolve this problem, we generated in separate experiments the molecule A from Fe(CO)<sub>5</sub> enriched in <sup>13</sup>CO, first to the extent of 25%, then of 50%, and finally of 83%. Random mixtures of the different isotopomers of A of the type Fe(<sup>12</sup>CO)<sub>x-n</sub>(<sup>13</sup>CO)<sub>n</sub> were presumed to be formed in this way. Figure 4 compares part of the IR spectrum observed for A 50% enriched in <sup>13</sup>CO (trace a) with the optimum spectra calculated on the basis of the different models, XII–XV, for a range of angles; the comparison is confined to the region between 2020 and 2180 cm<sup>-1</sup> where problems of overlap are least severe. There is not enough information to calculate independently bond angles and dipole derivative ratios, and so we have set all such ratios equal to unity; independent studies encourage us to believe that such an assumption is unlikely to be too wide of the mark. The best fits were achieved with the following angles: XII, θ = 220°; XIII, θ<sub>1</sub> = 120, θ<sub>2</sub> = 90°; XIV, θ<sub>1</sub> = 140, θ<sub>2</sub> = 120°. The vibrational problem with model XV is underdetermined, with no unique solution in terms of all three bond angles θ<sub>1</sub>, θ<sub>2</sub>, and θ<sub>3</sub>. We have therefore followed the example of the C<sub>s</sub> isomer of HMn(CO)<sub>4</sub><sup>31</sup> by assuming that θ<sub>1</sub> = θ<sub>2</sub>; the calculated spectrum depicted in

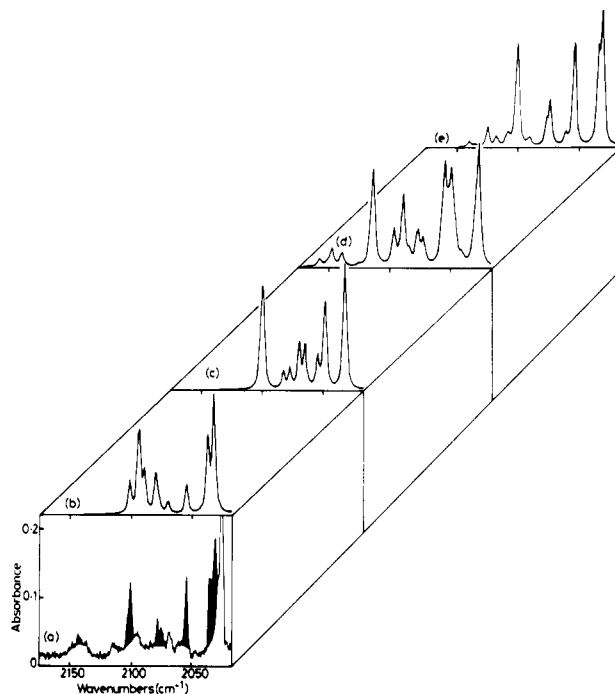


**Figure 4.** (a) IR spectrum observed for A 50% enriched in <sup>13</sup>CO showing the ν(C—O) region 2020–2180 cm<sup>-1</sup> (Ar:O<sub>2</sub>:Fe(CO)<sub>5</sub> = ca. 2000:100:1; photolysis for 40 min at λ = ca. 312 nm; bands due to A distinguished by black infilling). (b) Spectrum calculated for model XII with θ = 220°; k<sub>1</sub> = 1718.2, k<sub>2</sub> = 1757.8, k<sub>11</sub> = 50.0, and k<sub>12</sub> = 14.0 N m<sup>-1</sup>. (c) Spectrum calculated for model XIII with θ<sub>1</sub> = 120 and θ<sub>2</sub> = 90°; k<sub>1</sub> = 1708.1, k<sub>2</sub> = 1777.8, k<sub>11</sub> = 40.0, and k<sub>12</sub> = 9.9 N m<sup>-1</sup>. (d) Spectrum calculated for model XIV with θ<sub>1</sub> = 140 and θ<sub>2</sub> = 120°; k<sub>1</sub> = 1728.2, k<sub>2</sub> = 1796.5, k<sub>11</sub> = 60.0, k<sub>22</sub> = 13.1, and k<sub>12</sub> = 27.7 N m<sup>-1</sup>. (e) Spectrum calculated for model XV with θ<sub>1</sub> = θ<sub>2</sub> = 100 and θ<sub>3</sub> = 160°; k<sub>1</sub> = 1784.1, k<sub>2</sub> = 1749.9, k<sub>3</sub> = 1760.2, k<sub>12</sub> = 4.2, k<sub>13</sub> = 3.4, k<sub>22</sub> = 81.7, and k<sub>23</sub> = 28.1 N m<sup>-1</sup>.

Figure 4e corresponds to the bond angles θ<sub>1</sub> = θ<sub>2</sub> = 100 and θ<sub>3</sub> = 160°, together with the force constants k<sub>1</sub> = 1784.1, k<sub>2</sub> = 1749.9, k<sub>3</sub> = 1760.2, k<sub>12</sub> = 4.2, k<sub>13</sub> = 3.4, k<sub>22</sub> = 81.7, and k<sub>23</sub> = 28.1 N m<sup>-1</sup>. Although these do not represent a unique solution, the resulting model (XV) provides a considerably better account of the observed spectrum than do any of the others. Thus, model XII fails to reproduce the relative intensities of the absorptions near 2030 and 2050 cm<sup>-1</sup> and also gives but a poor account of the region near 2100 cm<sup>-1</sup> and model XIII implies the presence of an extra feature to high energy of the clearly defined singlet near 2050 cm<sup>-1</sup>, whereas model XIV suggests that there should be a doublet and not a singlet near 2050 cm<sup>-1</sup> and also gives a less than satisfactory account of the region 2060–2090 cm<sup>-1</sup>.

That A is a tetracarbonyl with the structure XV is endorsed by the results shown in Figure 5, where the scope of the measurements and calculations has been extended to accommodate degrees of <sup>13</sup>CO enrichment varying from 25 to 83%. In each case all the main features of the observed spectrum are matched closely by those predicted by our C<sub>s</sub> model with the geometry and force field specified above. Accordingly it appears that the geometry of the carbonyl fragment may be described as a square-pyramidal framework with a vacancy in the basal plane.

The discovery of such a fragment is not unduly surprising. Previous studies focusing on matrix-isolated HMn(CO)<sub>4</sub><sup>31</sup> and CH<sub>3</sub>Mn(CO)<sub>4</sub><sup>35</sup> have suggested in each case a square-pyramidal skeleton with the one-electron substituent located in the basal plane; photolysis is believed to induce isomerization to an apically substituted form. Structure XVI, which corresponds to the Mn(CO)<sub>4</sub> unit giving the best account of the IR spectrum of HMn(CO)<sub>4</sub>,<sup>31</sup> is strikingly similar to XV. Indeed, the IR spectrum of A shows an intensity pattern in the ν(C—O) region closely akin to those of HMn(CO)<sub>4</sub><sup>31</sup> and CH<sub>3</sub>Mn(CO)<sub>4</sub>,<sup>35</sup> although the bands occur at significantly higher energies in A than in the manganese compounds. On this evidence, the iron atom in A must be pre-

(44) Wu, Y.-M.; Bentsen, J. G.; Brinkley, C. G.; Wrighton, M. S. *Inorg. Chem.* **1987**, *26*, 530. Weiller, B. H.; Miller, M. E.; Grant, E. R. *J. Am. Chem. Soc.* **1987**, *109*, 352. Angermund, H.; Grevels, F.-W.; Moser, R.; Benn, R.; Krüger, C.; Romão, M. J. *Organometallics* **1988**, *7*, 1994.

(45) Grevels, F.-W.; Jacke, J.; Klotzbücher, W. E.; Krüger, C.; Seevogel, K.; Tsay, Y.-H. *Angew. Chem., Int. Ed. Engl.* **1987**, *26*, 885. Grevels, F.-W.; Jacke, J.; Seevogel, K. *J. Mol. Struct.* **1988**, *174*, 107.

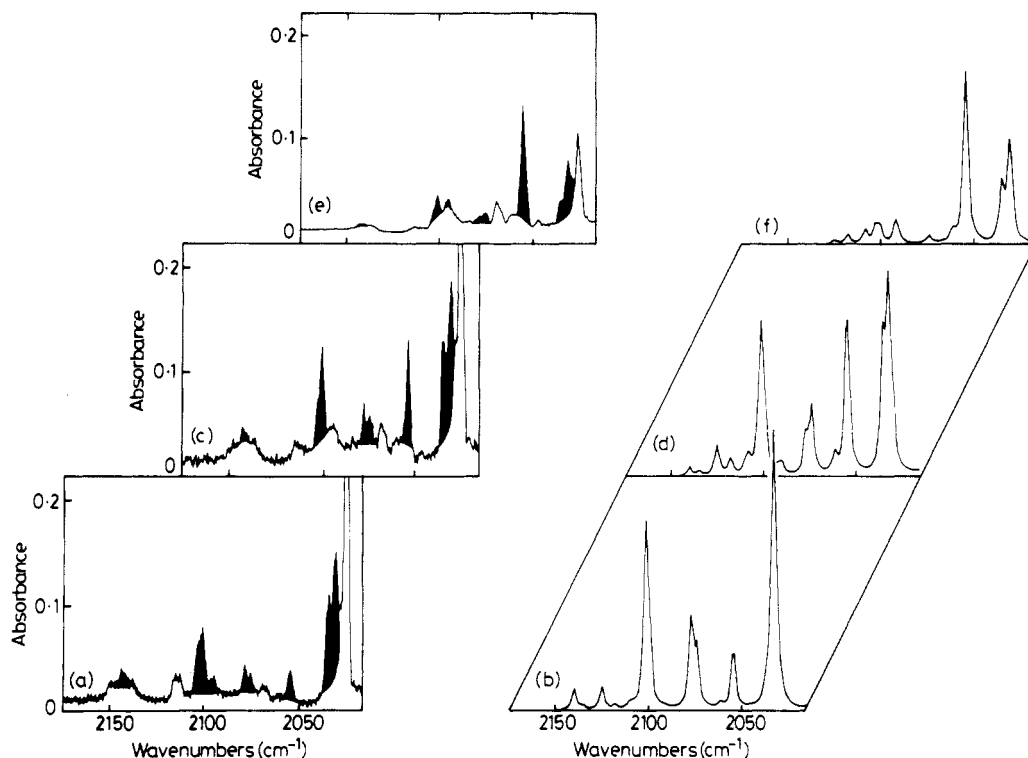
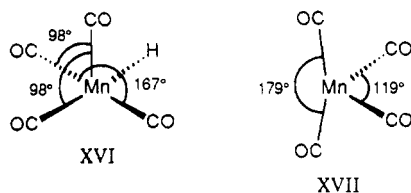


**Figure 5.** Stacked plot comparing the IR spectrum observed for A in the region 2020–2180  $\text{cm}^{-1}$  (bands marked by black infilling) with that predicted for model XV on the basis of the bond angles and force constants given previously (Figure 4): (a) observed and (b) predicted for 25%  $^{13}\text{CO}$  enrichment; (c) observed and (d) predicted for 50%  $^{13}\text{CO}$  enrichment; (e) observed and (f) predicted for 83%  $^{13}\text{CO}$  enrichment.

sumed to be in a formal oxidation state higher than the +1 of the manganese center in  $\text{XMn}(\text{CO})_4$  ( $\text{X} = \text{H}$  or  $\text{CH}_3$ ). Halogenomanganese(I) tetracarbonyls,  $\text{XMn}(\text{CO})_4$  ( $\text{X} = \text{Cl}, \text{Br}$ , or  $\text{I}$ ), have also been identified in matrix environments,<sup>36</sup> and these are noteworthy for the claim that they are each modeled on a trigonal bipyramid, e.g. XVII (with an equatorially sited one-electron ligand giving  $C_{2v}$  symmetry) rather than a square-based pyramid (with a basally sited one-electron ligand and  $C_s$  symmetry). The  $C_s$  structure is consistent with molecular orbital predictions for  $\text{HMn}(\text{CO})_4$ , and it has been suggested that the different structure adopted, for example, by  $\text{BrMn}(\text{CO})_4$ , is due to  $\pi$ -bonding effects, implicating the halogen ligand.<sup>46</sup> However, the potential energy surface reveals but a small barrier to interconversion between the two structures, and the balance could well hinge on the nature of the ligand coordinated to the  $\text{Mn}(\text{CO})_4$  fragment or even on the perturbing effect of the matrix environment.<sup>47</sup>



(b)  $\nu(\text{M}=\text{O})$  or  $\nu(\text{O}=\text{O})$  Region. In the region of the IR spectrum between 750 and 1100  $\text{cm}^{-1}$ , A shows just two absorptions, occurring at 914 and 885  $\text{cm}^{-1}$ . It is possible that these correspond to the symmetric and antisymmetric stretching modes of a bent  $\text{O}=\text{Fe}=\text{O}$  unit. If so, the relative intensities of the bands<sup>42</sup> indicate an  $\text{O}=\text{Fe}=\text{O}$  bond angle of about  $110^\circ$ . When A is generated in a matrix doped with  $^{18}\text{O}_2$ , in place of  $^{16}\text{O}_2$ , the

**Table IV.** IR Bands of A Observed in the Region 800–1000  $\text{cm}^{-1}$

band	wavenumber ( $\text{cm}^{-1}$ ) <sup>a</sup>				asymmetry parameter, $\rho^b$
	$^{16}\text{O}_2$	$^{16}\text{O}^{18}\text{O}$	$^{18}\text{O}_2$	$\Delta(^{16}\text{O}_2 - ^{18}\text{O}_2)$	
1	914	894	875	39	1.02
2	885	868	849	36	0.95

<sup>a</sup> Refers to  $\text{O}_2$ -doped Ar matrices at ca. 20 K; error limits  $\pm 1 \text{ cm}^{-1}$ .

<sup>b</sup>  $\rho = 2[\nu(^{16}\text{O}_2) - \nu(^{16}\text{O}^{18}\text{O})]/[\nu(^{16}\text{O}_2) - \nu(^{18}\text{O}_2)]$  (see refs 11–13).

two bands move to 875 and 849  $\text{cm}^{-1}$ ; the  $^{16}\text{O}$ – $^{18}\text{O}$  shifts of 39 and 36  $\text{cm}^{-1}$ , respectively, are also reasonable for a dioxoiron unit,<sup>10–13,18,41,48</sup> while appearing to be too small to be assigned to the  $\nu(\text{O}=\text{O})$  fundamental of a unit like I or II. As illustrated in Figure 6, however, this interpretation runs into a serious problem, namely the *reversal of the relative intensities* of the two bands brought about by  $^{18}\text{O}$  substitution. Thus, for the  $^{16}\text{O}$  version of A the ratio  $I_{914}:I_{885}$  is 2.1:1; for the  $^{18}\text{O}$  version of A the corresponding ratio  $I_{875}:I_{849}$  is 1:3. There are few effects likely to cause such a change in the intensity of one band relative to an adjacent one, but one obvious mechanism hinges on Fermi resonance.

There are two possible bases for Fermi resonance in A. One involves the first overtone of one of the  $\nu(\text{Fe}=\text{O})$  fundamentals and the  $a_1$  fundamental  $\nu(\text{O}=\text{O})$  of a peroxoiron fragment,  $(\eta^2\text{-O}_2)\text{Fe}$  (II); the other involves the first overtone of the bending mode  $\delta(\text{FeO}_2)$  and the  $a_1$  fundamental  $\nu(\text{Fe}=\text{O})$  of a dioxoiron fragment,  $\text{O}=\text{Fe}=\text{O}$  (IV). The change of intensity, and uncharacteristic isotopic shifts, can then be attributed to a change in the degree of interaction between the two vibrational states, reflecting the different responses of the relevant high- and low-energy fundamentals to  $^{18}\text{O}$  enrichment. Just such an effect has been observed in the case of the matrix-isolated molecule  $\text{SNO}$ .<sup>49</sup> Of the two possibilities ventured for A the second seems less likely than the first because it would not obviously account for the apparent absence from the spectrum of the  $b_2$  mode corresponding to the antisymmetric  $\text{O}=\text{Fe}=\text{O}$  stretching fundamental which

(46) Burdett, J. K. *Inorg. Chem.* **1976**, *15*, 212. Lichtenberger, D. L.; Brown, T. L. *J. Am. Chem. Soc.* **1978**, *100*, 366. Berke, H.; Hoffmann, R. *J. Am. Chem. Soc.* **1978**, *100*, 7224.

(47) Arthers, S. A.; Beattie, I. R.; Jones, P. J. *J. Chem. Soc., Dalton Trans.* **1984**, 711. Beattie, I. R.; Millington, K. R. *J. Chem. Soc., Dalton Trans.* **1987**, 1521. Beattie, I. R.; Jones, P. J.; Millington, K. R.; Willson, A. D. *J. Chem. Soc., Dalton Trans.* **1988**, 2759. Ogden, J. S.; Levason, W.; Hope, E. G.; Graham, J. T.; Jenkins, D. M.; Angell, R. M. *J. Mol. Struct.* **1990**, *222*, 109.

(48) Hewett, W. D., Jr.; Newton, J. H.; Weltner, W., Jr. *J. Phys. Chem.* **1975**, *79*, 2640.

(49) Hawkins, M.; Downs, A. J. *J. Phys. Chem.* **1984**, *88*, 3042.



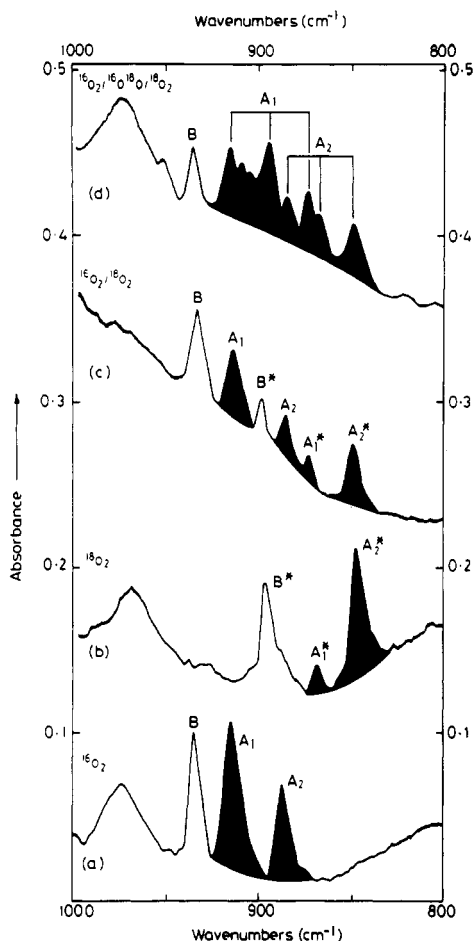


**Figure 6.** IR spectrum of A in the region 800–1000  $\text{cm}^{-1}$  (bands marked by black infilling are due wholly or mainly to A): (a) for a sample generated from  $^{16}\text{O}_2$ ; (b) for a sample generated from  $^{18}\text{O}_2$ ; (c) for a sample generated from a mixture of  $^{16}\text{O}_2$  and  $^{18}\text{O}_2$  ( $^{16}\text{O}_2$ : $^{18}\text{O}_2$  = 3:2); (d) for a sample generated from a mixture of  $^{16}\text{O}_2$ ,  $^{16}\text{O}^{18}\text{O}$ , and  $^{18}\text{O}_2$  ( $^{16}\text{O}_2$ : $^{16}\text{O}^{18}\text{O}$ : $^{18}\text{O}_2$  = 1:2:1). The subscripts 1 and 2 are used to denote the two distinct bands due to A and the asterisks to denote bands due to  $\text{Fe}^{18}\text{O}_x$  species.

is expected to be *stronger* in IR absorption than its symmetric ( $a_1$ ) counterpart. In either case there should be a fundamental near  $1/4(914 + 885) = 450 \text{ cm}^{-1}$  in the  $^{16}\text{O}$  version of the molecule. Careful scrutiny of the spectrum did reveal a very weak feature near  $425 \text{ cm}^{-1}$ , but whether this corresponds to the “missing” fundamental must be open to doubt.

More positive conclusions favoring a peroxo- rather than a dioxometal structure for A come from experiments utilizing a scrambled mixture of the dioxygen isotopomers  $^{16}\text{O}_2$ ,  $^{16}\text{O}^{18}\text{O}$ , and  $^{18}\text{O}_2$ . In this case, two *symmetrical* triplets (with asymmetry parameters<sup>11–13</sup> of 1.02 and 0.95, respectively) are observed to take the place of the bands appearing at 914 and 885  $\text{cm}^{-1}$ ; the wavenumbers of the relevant bands are listed in Table IV. Such a symmetrical pattern argues not for a dioxometal but for a peroxometal unit analogous to that in molecules like  $(\eta^2\text{-O}_2)\text{M}(\text{CO})_4$  (where M = Cr, Mo, or W).<sup>12,50–52</sup> Thus, the most likely interpretation is that A is peroxoiron tetracarbonyl,  $(\eta^2\text{-O}_2)\text{Fe}(\text{CO})_4$ , wherein the peroxo group occupies the basal plane of what approximates to a square-based pyramid (XVIII). The compound is thus formally a tetracarbonyl of iron(II). As such, it is iso-electronic, and therefore likely to be isostructural, with the

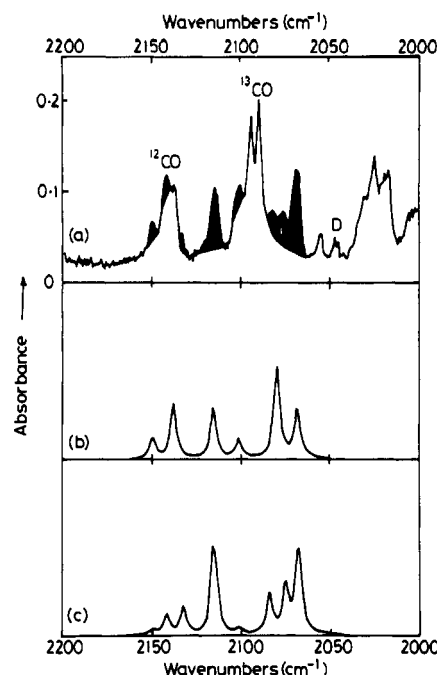
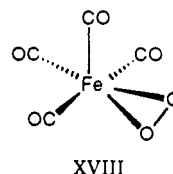


**Figure 7.** IR spectrum of B 50% enriched in  $^{13}\text{CO}$  showing the  $\nu(\text{C—O})$  region: (a) spectrum observed after 300 min of photolysis at  $\lambda = \text{ca. } 312 \text{ nm}$  ( $\text{Ar}:\text{O}_2:\text{Fe}(\text{CO})_5 = \text{ca. } 1000:50:1$ ; product bands marked by black infilling); (b) spectrum calculated for model XIX with  $\phi = 70^\circ$  and  $k_{\text{CO}} = 1837.3$  and  $k_{\text{CO,CO}} = 29.1 \text{ N m}^{-1}$ ; (c) spectrum calculated for model XX with  $\phi = 70^\circ$  and  $k_{\text{CO}} = 1827.5$  and  $k_{\text{CO,CO}} = 19.5 \text{ N m}^{-1}$ .

manganese(I) tetracarbonyls  $\text{CH}_3\text{Mn}(\text{CO})_4$ ,<sup>35</sup>  $\text{HMn}(\text{CO})_4$ ,<sup>31</sup> and  $\text{ClMn}(\text{CO})_4$ .<sup>36</sup>



If A is to be regarded as an  $\text{O}_2$  adduct of  $\text{Fe}(\text{CO})_4$ , it stands in marked contrast to oxyhemoglobin, oxymyoglobin, and their numerous model compounds.<sup>2,8,9,53</sup> All the spectroscopic and structural evidence on these iron(II) porphyrin adducts points to end-on coordination of the  $\text{O}_2$  ligand with an  $\text{Fe—O—O}$  angle near  $130^\circ$  (i.e. a superoxoiron unit of the type I). In keeping with this formulation, the  $\nu(\text{O—O})$  vibration occurs at an energy ( $1100\text{--}1220 \text{ cm}^{-1}$ ) much higher than the corresponding mode of A. Intriguingly, however, oxyhemoglobin itself is reported to show not one but two IR bands in the  $\nu(\text{O—O})$  region, an observation which has been interpreted on the basis of Fermi resonance between the  $\nu(\text{O—O})$  fundamental and the first overtone of the  $\nu(\text{Fe—O}_2)$  fundamental.<sup>54</sup> Hence our interpretation of the spectrum of A in the region  $800\text{--}1000 \text{ cm}^{-1}$  is not without precedent.

**3.3. Intermediate B. (a)  $\nu(\text{C—O})$  Region.** Intermediate B is characterized by two  $\nu(\text{C—O})$  fundamentals centered at 2149 and 2115  $\text{cm}^{-1}$ . Since the average wavenumber of these modes ( $2132 \text{ cm}^{-1}$ ) is somewhat higher than that ( $2088 \text{ cm}^{-1}$ ) of the corresponding modes of A, it seems reasonable to suppose that the metal center in B has a higher formal oxidation state than that in A. Moreover, the observation of two  $\nu(\text{C—O})$  fundamentals in the IR spectrum of B argues in favor of either a non-linear iron

(50) Horn, R. W.; Weissberger, E.; Collman, J. P. *Inorg. Chem.* **1970**, *9*, 2367.

(51) Nakamura, A.; Tatsuno, Y.; Yamamoto, M.; Otsuka, S. *J. Am. Chem. Soc.* **1971**, *93*, 6052.

(52) Huber, H.; Klotzbücher, W.; Ozin, G. A.; Vander Voet, A. *Can. J. Chem.* **1973**, *51*, 2722.

(53) Watanabe, T.; Ama, T.; Nakamoto, K. *J. Phys. Chem.* **1984**, *88*, 440. Bajdor, K.; Oshio, H.; Nakamoto, K. *J. Am. Chem. Soc.* **1984**, *106*, 7273. Wagner, W.-D.; Paeng, I. R.; Nakamoto, K. *J. Am. Chem. Soc.* **1988**, *110*, 5565.

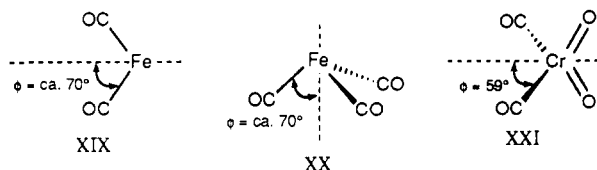
(54) Caughey, W. S.; Choc, M. G.; Houtchens, R. A. In *Biochemical and Clinical Aspects of Oxygen*; Caughey, W. S., Ed.; Academic Press: New York, 1979; p 1.

**Table V.**  $\nu(\text{C}=\text{O})$  Modes of Different  $^{12}\text{CO}/^{13}\text{CO}$  Isotopomers of B Isolated in an  $\text{O}_2$ -Doped Ar Matrix at ca. 20 K: Wavenumbers ( $\text{cm}^{-1}$ ) Observed and Calculated for a Pyramidal  $\text{Fe}(\text{CO})_3$  Fragment

obsd	calcd <sup>c</sup>	mode	molecule
2149 <sup>a</sup>	2149.4	$a_1$	$\text{Fe}(^{12}\text{CO})_3$
2115 <sup>a</sup>	2115.6	$e$	
2141 <sup>b</sup>	2142.1	$a_1$	
2115 <sup>a</sup>	2115.6	$b_2$	$\text{Fe}(^{12}\text{CO})_2(^{13}\text{CO})$
2076 <sup>a</sup>	2075.5	$a_1$	
2134 <sup>a</sup>	2132.8	$a_1$	$\text{Fe}(^{12}\text{CO})(^{13}\text{CO})_2$
2080 <sup>b</sup>	2084.6	$a_1$	
2069 <sup>a</sup>	2068.4	$b_2$	
2102 <sup>a</sup>	2101.5	$a_1$	$\text{Fe}(^{13}\text{CO})_3$
2069 <sup>a</sup>	2068.4	$e$	

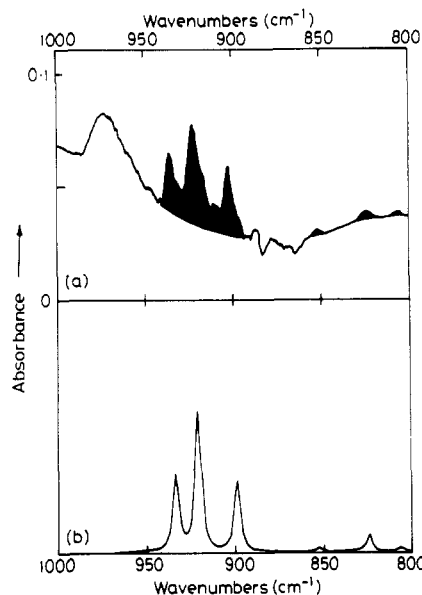
<sup>a</sup>Error limits  $\pm 1 \text{ cm}^{-1}$ . <sup>b</sup>Error limits  $\pm 4 \text{ cm}^{-1}$ . <sup>c</sup>Calculated on the assumption of an energy-factored force field for an  $\text{Fe}(\text{CO})_3$  unit with  $C_{3v}$  symmetry and a semivertical angle  $\phi = 70^\circ$  (XX);  $k_{\text{CO}} = 1827.5$  and  $k_{\text{CO,CO}} = 19.45 \text{ N m}^{-1}$ .

dicarbonyl constituent with  $C_{2v}$  symmetry (XIX) or a pyramidal iron tricarbonyl constituent with  $C_{3v}$  symmetry (XX). The relative intensities of the two bands are difficult to estimate because of problems of overlap but point to a semivertical angle,  $\phi$ , subtended by the CO oscillators of either model in the order of  $70^\circ$ .<sup>39,42</sup> This may be compared with the value of  $59^\circ$  estimated for the corresponding angle of the matrix-isolated molecule  $\text{O}_2\text{Cr}(\text{CO})_2$  (XXI).<sup>10</sup>



It is a relatively straightforward procedure to distinguish between the models XIX and XX by partially enriching B in  $^{13}\text{CO}$  and comparing the energies and intensities of the resulting absorptions with those calculated for each of the two models. Our experiments showed that  $^{13}\text{CO}$  enrichment of B gives new bands at or near 2140, 2102, 2080, and 2069  $\text{cm}^{-1}$ . As shown in Table V and Figure 7, the features of the spectrum are much more closely in accord with the predictions of model XX than with those of model XIX. Features near 2140 and 2080  $\text{cm}^{-1}$  assigned exclusively to the mixed  $^{12}\text{CO}/^{13}\text{CO}$  isotopomers were in practice partially obscured by the absorptions of free CO, but the most telling evidence against the  $\text{Fe}(\text{CO})_2$  formulation comes from the relative weakness of these features compared with the pairs of flanking bands at 2149/2115 and 2102/2069  $\text{cm}^{-1}$  originating wholly or mainly in the all- $^{12}\text{CO}$  and all- $^{13}\text{CO}$  isotopomers, respectively (see Figure 7).<sup>55</sup>

**(b)  $\nu(\text{M}=\text{O})$  or  $\nu(\text{O}=\text{O})$  Region.** In this region of the IR spectrum there is readily discernible only one absorption which can be attributed with confidence to B, and it occurs at 934  $\text{cm}^{-1}$ . In addition, however, there is a second very weak band at 851  $\text{cm}^{-1}$  whose growth and decay characteristics suggest that it too probably belongs to B. When B is generated in an argon matrix doped with  $^{18}\text{O}_2$ , rather than  $^{16}\text{O}_2$ , the absorptions shift to 899 and 806  $\text{cm}^{-1}$ , respectively. The magnitudes of the  $^{16}\text{O}$ - $^{18}\text{O}$  shifts (35 and 45  $\text{cm}^{-1}$ ) are in line with those observed for molecules containing a dioxometal moiety,  $\text{O}=\text{M}=\text{O}$ .<sup>10-13,18,41,48</sup> It seems reasonable therefore to postulate that B contains an  $\text{O}=\text{Fe}=\text{O}$  fragment. The experimental results then provide for an estimate of the  $\text{O}=\text{Fe}=\text{O}$  bond angle on the basis of (i) the  $^{16}\text{O}$ - $^{18}\text{O}$  shift of the

**Figure 8.** IR spectrum of B in the region 800–1000  $\text{cm}^{-1}$ : (a) observed spectrum for a sample generated from a scrambled mixture of the isotopomers  $^{16}\text{O}_2$ ,  $^{16}\text{O}^{18}\text{O}$ , and  $^{18}\text{O}_2$  (in the proportions 1:2:1; product bands marked by black infilling); (b) spectrum predicted for the  $\nu(\text{Fe}=\text{O})$  modes of an angular  $\text{O}=\text{Fe}=\text{O}$  unit (XXII) with the bond angle and force constants as in Table VI.**Table VI.** IR Bands of B in the Region 800–1000  $\text{cm}^{-1}$ : Wavenumbers ( $\text{cm}^{-1}$ ) Observed and Calculated for the  $\nu(\text{Fe}=\text{O})$  Modes of an Angular  $\text{O}=\text{Fe}=\text{O}$  Fragment

obsd <sup>a</sup>	calcd <sup>b</sup>	mode	molecule
934	934.0	$\nu_{\text{as}}(\text{FeO}_2)$ ( $b_2$ )	$\text{Fe}^{16}\text{O}_2$
921	920.9	$\nu_{\text{as}}(\text{FeO}_2)$ ( $a'$ )	$\text{Fe}^{16}\text{O}^{18}\text{O}$
899	899.1	$\nu_{\text{as}}(\text{FeO}_2)$ ( $b_2$ )	$\text{Fe}^{18}\text{O}_2$
851	851.1	$\nu_{\text{s}}(\text{FeO}_2)$ ( $a_1$ )	$\text{Fe}^{16}\text{O}_2$
824	823.9	$\nu_{\text{s}}(\text{FeO}_2)$ ( $a'$ )	$\text{Fe}^{16}\text{O}^{18}\text{O}$
806	805.3	$\nu_{\text{s}}(\text{FeO}_2)$ ( $a_1$ )	$\text{Fe}^{18}\text{O}_2$

<sup>a</sup>Refers to  $\text{O}_2$ -doped Ar matrices at ca. 20 K; error limits  $\pm 2 \text{ cm}^{-1}$ . <sup>b</sup>Based on a  $C_{2v}$   $\text{O}=\text{Fe}=\text{O}$  unit with a bond angle of  $142^\circ$  and an energy-factored force field for the  $\nu(\text{Fe}=\text{O})$  modes with the force constants  $k_{\text{FeO}} = 593.8$  and  $k_{12} = 50 \text{ N m}^{-1}$  (see refs 10, 48, and 56).

antisymmetric  $\nu(\text{Fe}=\text{O})$  mode and (ii) the relative intensities of the symmetric and antisymmetric  $\nu(\text{Fe}=\text{O})$  modes in IR absorption. The  $^{16}\text{O}$ - $^{18}\text{O}$  shift of 35  $\text{cm}^{-1}$  suggests an upper limit to the bond angle of  $142_{-11}^{+19^\circ}$ , while the measured intensity ratio  $I_{\text{antisym}}:I_{\text{sym}} = 20\text{--}40:1$  suggests an angle near  $150^\circ$ . Hence the  $\text{O}=\text{Fe}=\text{O}$  bond angle is probably in the range  $140\text{--}160^\circ$ .

Confirmation that B does indeed contain a nonlinear  $\text{O}=\text{Fe}=\text{O}$  fragment comes from the IR spectrum of the intermediate generated in an argon matrix doped with a scrambled mixture of  $^{16}\text{O}_2$ ,  $^{16}\text{O}^{18}\text{O}$ , and  $^{18}\text{O}_2$ . As shown in Figure 8 and itemized in Table VI, an *unsymmetrical* triplet of bands was observed, with components at 934, 921, and 899  $\text{cm}^{-1}$  and an asymmetry parameter of 0.74,<sup>11-13</sup> corresponding to the antisymmetric  $\nu(\text{Fe}=\text{O})$  modes of the three  $^{16}\text{O}/^{18}\text{O}$  isotopomers of B. A weak feature at 824  $\text{cm}^{-1}$ , which may well belong to  $\nu_{\text{sym}}(\text{Fe}=\text{O})$  of the  $^{16}\text{O}^{18}\text{O}$  version of B (the most abundant of the three isotopomers), was also identified. The results can be simulated remarkably well by a very simple vibrational model in which the  $\nu(\text{Fe}=\text{O})$  modes of an angular  $\text{O}=\text{Fe}=\text{O}$  moiety are factored off from the remaining vibrations.<sup>10,48,56</sup>

Taken together, the various pieces of evidence leave little doubt that B is dioxoiron tricarbonyl,  $\text{O}_2\text{Fe}(\text{CO})_3$ , an analog of "chromyl carbonyl",<sup>10</sup> and that it has the structure XXII. That it is a carbonyl derivative of iron in the formal oxidation state +4 is supported by the unusually high energy of the  $\nu(\text{C}=\text{O})$  fundamentals (with a mean value only about 14  $\text{cm}^{-1}$  less than that of

(55) An  $\text{Fe}(\text{CO})_3$  unit with  $C_{2v}$  symmetry (XII) or  $C_s$  symmetry (XIII) is characterized by a three-band IR spectrum in which the two features at lower energy are typically almost degenerate (see Figure 3 and refs 44 and 45). Hence we cannot, on the evidence of the all- $^{12}\text{CO}$  spectrum alone, strictly rule out the possibility of a tricarbonyl fragment with lower than  $C_{3v}$  symmetry. However, a model with  $C_{2v}$  symmetry or one showing marked departure from  $C_{3v}$  toward  $C_s$  symmetry is found wanting in its ability to reproduce the effects of  $^{13}\text{CO}$  enrichment (on much the same sort of grounds as the  $C_{2v}$  dicarbonyl model proves to be inadequate).

(56) Ogden, J. S.; Williams, S. J. *J. Chem. Soc., Dalton Trans.* **1982**, 825.

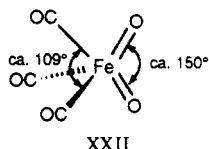
**Table VII.** IR Bands of C in the Region 800–1000  $\text{cm}^{-1}$ : Wavenumbers ( $\text{cm}^{-1}$ ) Observed and Calculated for the  $\nu(\text{Fe}=\text{O})$  Modes of an Angular  $\text{O}=\text{Fe}=\text{O}$  Fragment

obsd <sup>a</sup>	calcd <sup>b</sup>	mode	molecule
929	929.5	$\nu_{\text{as}}(\text{FeO}_2)$ ( $b_2$ )	$\text{Fe}^{16}\text{O}_2$
918	918.0	$\nu_{\text{as}}(\text{FeO}_2)$ ( $a'$ )	$\text{Fe}^{16}\text{O}^{18}\text{O}$
895	894.5	$\nu_{\text{as}}(\text{FeO}_2)$ ( $b_2$ )	$\text{Fe}^{18}\text{O}_2$
874	873.5	$\nu_s(\text{FeO}_2)$ ( $a_1$ )	$\text{Fe}^{16}\text{O}_2$
844	844.3	$\nu_s(\text{FeO}_2)$ ( $a'$ )	$\text{Fe}^{16}\text{O}^{18}\text{O}$
828	826.9	$\nu_s(\text{FeO}_2)$ ( $a_1$ )	$\text{Fe}^{18}\text{O}_2$

<sup>a</sup> Refers to  $\text{O}_2$ -doped Ar matrices at ca. 20 K; error limits  $\pm 2 \text{ cm}^{-1}$ .

<sup>b</sup> Based on a  $\text{C}_{2v}$   $\text{O}=\text{Fe}=\text{O}$  unit with a bond angle of  $139^\circ$  and an energy-factored force field for the  $\nu(\text{Fe}=\text{O})$  modes with the force constants  $k_{\text{FeO}} = 607$  and  $k_{12} = 65 \text{ N m}^{-1}$ .

free  $\text{CO}$ ,<sup>32</sup> cf.  $\text{O}_2\text{Cr}(\text{CO})_2^{10}$  for which the corresponding shift is about  $46 \text{ cm}^{-1}$ ).



Iron chemistry holds few known parallels to this molecule. The binary iron(IV) oxide  $\text{O}=\text{Fe}=\text{O}$  has been described as one of the products formed by the interaction of  $\text{O}_2$  molecules with iron atoms in an argon matrix,<sup>16</sup> but the spectroscopic evidence is far from compelling. Although the corresponding chromium(IV) derivative,  $\text{O}=\text{Cr}=\text{O}$ , is the ultimate metal-containing product derived from photooxidation of matrix-isolated  $\text{Cr}(\text{CO})_6$ ,<sup>13,18</sup> we found no evidence to support the formation of a similar species on prolonged UV photolysis of  $\text{Fe}(\text{CO})_5$  in the presence of  $\text{O}_2$ .<sup>34</sup> However, the results of our experiments show that B is highly susceptible to further change, its decay being induced not only by photolysis but also by thermal means (e.g. raising the matrix temperature to about 33 K). The likely significance of this finding is discussed in section 4.

**3.4. Intermediate C.** Continued irradiation of the matrix at wavelengths near 312 nm results in the decay of B and the appearance and growth of the intermediates C, D, and E; the buildup of these new intermediates at the expense of B is also favored by annealing of the matrix. Intermediate C shows but one band in the  $\nu(\text{C}=\text{O})$  region of its IR spectrum (at  $2120 \text{ cm}^{-1}$ ), a shoulder near  $929 \text{ cm}^{-1}$  on the low-frequency flank of the band at  $934 \text{ cm}^{-1}$  associated with B, and the suggestion of a weak band near  $874 \text{ cm}^{-1}$ . On partial enrichment with  $^{13}\text{CO}$ , C gives rise to only two bands in the high-frequency region, namely at  $2120$  and  $2072 \text{ cm}^{-1}$ . The absence of any features arising from "mixed" species containing both  $^{12}\text{CO}$  and  $^{13}\text{CO}$  ligands causes us to believe that C is an iron monocarbonyl derivative.

The shoulder at  $929 \text{ cm}^{-1}$  shifts to  $895 \text{ cm}^{-1}$  when C is generated in an argon matrix in which  $^{16}\text{O}_2$  has given place to  $^{18}\text{O}_2$ . The magnitude of the  $^{16}\text{O}-^{18}\text{O}$  shift ( $35 \text{ cm}^{-1}$ ) is again consistent with the assignment of this feature to the antisymmetric  $\nu(\text{Fe}=\text{O})$  fundamental of an  $\text{O}=\text{Fe}=\text{O}$  unit, with an upper limit for the bond angle of  $139^{+17}_{-11}^\circ$ . The weak absorption near  $874 \text{ cm}^{-1}$  associated with the  $^{16}\text{O}$  version of C is then the obvious candidate for the symmetric  $\nu(\text{Fe}=\text{O})$  fundamental, the ratio of the intensities  $I_{929}/I_{870} = \text{ca. } 30:1$  suggesting a bond angle in the order of  $150^\circ$ .

Further evidence that C does indeed contain a dioxoiron moiety comes from an experiment in which C was generated in an argon matrix containing a scrambled mixture of  $^{16}\text{O}_2$ ,  $^{16}\text{O}^{18}\text{O}$ , and  $^{18}\text{O}_2$ . The spectrum was necessarily complicated by the proximity of the absorptions due to B and by the impossibility of producing significant concentrations of C in the absence of B (see Figure 2). As shown in Figure 9, however, it was possible to discern the features of an *unsymmetrical* triplet of bands, with an asymmetry parameter<sup>11–13</sup> of 0.69 and the components partially overlapping the members of the corresponding triplet identified with B. Table VII lists the observed and calculated wavenumbers for the relevant absorptions of C in this region of the spectrum. Despite the

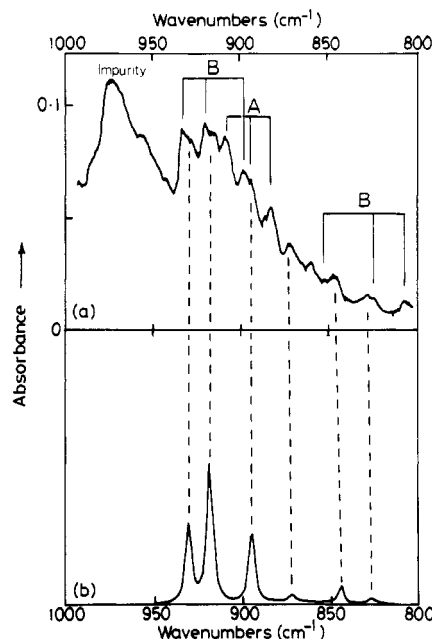
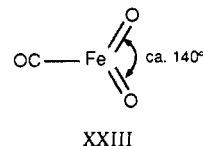


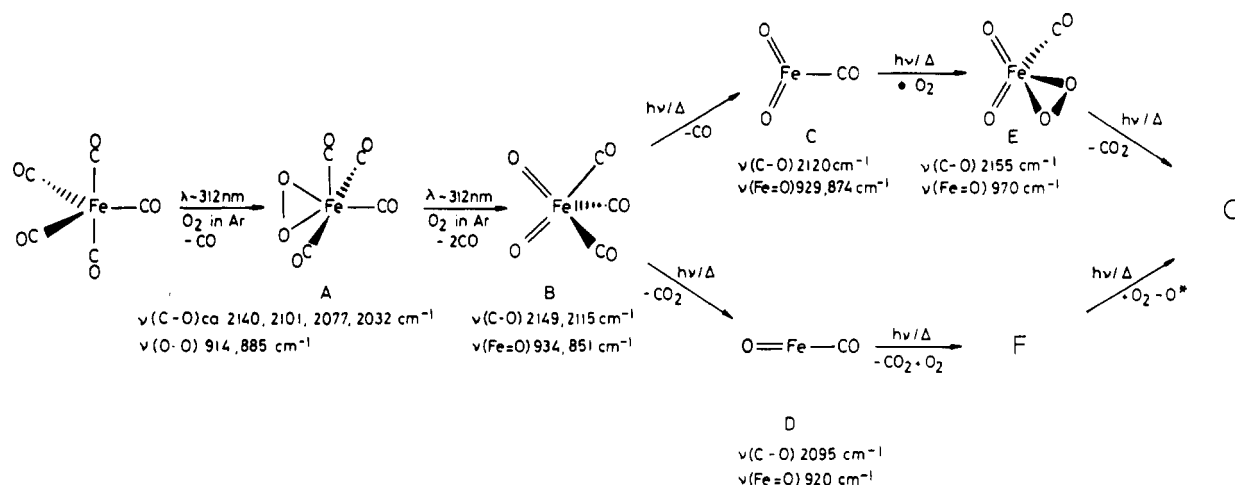
**Figure 9.** IR spectrum of C in the region 800–1000  $\text{cm}^{-1}$ : (a) spectrum exhibited by a matrix sample containing a scrambled mixture of the isotopomers  $^{16}\text{O}_2$ ,  $^{16}\text{O}^{18}\text{O}$ , and  $^{18}\text{O}_2$  ( $^{16}\text{O}_2:^{16}\text{O}^{18}\text{O}:^{18}\text{O}_2 = 1:2:1$ ;  $\text{Ar}:\text{O}_2:\text{Fe}(\text{CO})_5 = 1000:50:1$ ) after 400 min of photolysis at  $\lambda = \text{ca. } 312 \text{ nm}$ ; (b) spectrum predicted for the  $\nu(\text{Fe}=\text{O})$  modes of an angular  $\text{O}=\text{Fe}=\text{O}$  unit (XXIII) with the bond angle and force constants as in Table VII.

problems posed by the comparatively low concentrations and by partial masking of the IR bands by those of more abundant matrix components, all the evidence available leads to the same inference, namely that C is dioxoiron monocarbonyl (XXIII).



**3.5. Intermediates D and E.** On prolonged photolysis of an  $\text{O}_2$ -doped argon matrix containing iron pentacarbonyl with radiation having wavelengths near 312 nm—typically for more than 500 min—IR bands due to two minor intermediates D and E were found to appear and grow. At no stage was either of these intermediates found in significant yield, and the low intensities of their IR bands made it extremely difficult to arrive at a definitive identification. It seems likely, however, that both compounds are monocarbonyls. Thus, D displays just one band in the  $\nu(\text{C}=\text{O})$  region of the IR spectrum. This occurs at  $2095 \text{ cm}^{-1}$  and gives rise to only one other band (at  $2046 \text{ cm}^{-1}$ ) on partial  $^{13}\text{CO}$  enrichment, with no hint of any bands due to mixed  $^{12}\text{CO}/^{13}\text{CO}$  isotopomers. E is also characterized by a single weak feature in the  $\nu(\text{C}=\text{O})$  region, namely at  $2155 \text{ cm}^{-1}$ ; that no  $^{13}\text{CO}$  counterpart could be detected on  $^{13}\text{CO}$  enrichment is probably due to the inherent weakness of the feature and compounded by the masking effect of stronger absorptions due to other matrix components.

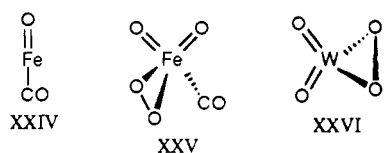
In the region of the IR spectrum between 800 and  $1000 \text{ cm}^{-1}$ , D shows a weak, sharp band at  $920 \text{ cm}^{-1}$  which grows as the bands due to B decay. The presence in the same neighborhood of stronger absorptions due to other species made it difficult to assess with certainty the effects of  $^{18}\text{O}$  enrichment of D, but the band at  $920 \text{ cm}^{-1}$  appeared to shift to  $882 \text{ cm}^{-1}$ . No feature attributable to an isotopomer of D containing *both*  $^{16}\text{O}$  and  $^{18}\text{O}$  could be identified, although it could easily have been obscured by other absorptions. The spectroscopic characteristics of E were, if anything, even harder to pin down than those of D. However, E appeared to give rise to an absorption at  $970 \text{ cm}^{-1}$  which shifted to  $935 \text{ cm}^{-1}$  on  $^{18}\text{O}$  substitution.

Scheme I. Photochemistry of the Matrix-Isolated System  $\text{Fe}(\text{CO})_5/\text{O}_2$  following Irradiation at Wavelengths Near 312 nm<sup>a</sup>

<sup>a</sup>The identities of the iron oxide molecules F and G will be revealed in part 2.

Although it is impossible on the basis of these observations to identify positively the intermediates D and E, the signs are that both are monocarbonyls. D may be a dioxoiron species, but the weight of the evidence—and particularly the energy of the  $\nu(\text{C}-\text{O})$  mode—are more consistent with its being a monooxoiron species, possibly with the structure XXIV. At 920  $\text{cm}^{-1}$ , the  $\nu(\text{Fe}=\text{O})$  mode of D is appreciably higher in energy than the vibrational fundamental of the matrix-isolated  $\text{FeO}$  molecule (873  $\text{cm}^{-1}$ ).<sup>14,16</sup> If our identification is correct, D resembles the iron(II) compounds  $(\eta^2\text{-C}_2\text{H}_4)\text{FeO}$  and  $\text{N}_2\text{FeO}$  recently brought to light by IR studies of the thermal and photochemical reactions involving iron atoms in low-temperature matrices,<sup>17</sup> and the  $\nu(\text{Fe}=\text{O})$  modes of these are reported to occur at 862.7 and 887.3  $\text{cm}^{-1}$ , respectively. Although the energies are again significantly lower than that of the  $\nu(\text{Fe}=\text{O})$  mode we attribute tentatively to  $\text{OCFeO}$  (XXIV), it is noticeable that  $\nu(\text{Fe}=\text{O})$  moves to higher energy when  $\text{FeO}$  is coordinated to a molecule able, like  $\text{N}_2$ , to transfer electron density to the metal center. Since  $\text{CO}$  is superior to  $\text{N}_2$  as an electron donor, it is not unreasonable that  $\nu(\text{Fe}=\text{O})$  for  $\text{OCFeO}$  should occur at an energy  $>887 \text{ cm}^{-1}$ . By contrast, iron(IV) “ferryl” derivatives like  $(\text{TPP})\text{FeO}$  (TPP = tetraphenylporphyrinato) and  $(\text{TpivPP})(\text{THF})\text{FeO}$  (TpivPP = tetrakis(*o*-pivaloylphenyl)porphyrinato; THF = tetrahydrofuran)<sup>57</sup> exhibit  $\nu(\text{Fe}=\text{O})$  vibrations at appreciably lower energies (800–860  $\text{cm}^{-1}$ ).

The unusually high energy of the  $\nu(\text{C}-\text{O})$  band of E (exceeding that of free  $\text{CO}$ <sup>32</sup>) argues not only for an extremely weak  $\text{Fe}\cdots\text{CO}$  interaction but also for a metal center in a formal oxidation state higher than that in any of the other oxoiron carbonyl intermediates (A, +2; B, +4; C, +4; D, +2). One possibility is that E has the structure XXV, which is akin to that of  $(\eta^2\text{-O}_2)\text{WO}_2$  (XXVI) generated by the matrix photooxidation of  $\text{W}(\text{CO})_6$ ,<sup>12,13</sup> and incorporating an iron(VI) center. Less likely is the possibility that E is  $\text{O}_3\text{FeCO}$ , since the low-frequency band of E shows a response to  $^{18}\text{O}$  enrichment quite different from that of the iron(VI) oxide molecule  $\text{FeO}_3$ , which we show to be one of the ultimate products of photooxidation.<sup>34</sup> The low-frequency band of E is very close

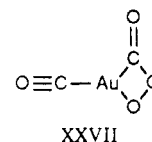


to that attributed elsewhere<sup>16</sup> to the antisymmetric  $\nu(\text{Fe}=\text{O})$  fundamental of a linear  $\text{O}=\text{Fe}=\text{O}$  molecule as trapped in an

argon matrix, and its  $^{16}\text{O}$ – $^{18}\text{O}$  isotopic shift implies a similar origin, with an upper limit of ca. 169° to the  $\text{O}=\text{Fe}=\text{O}$  bond angle.

#### 4. Conclusions

Drawing on the cumulative evidence presented in this paper, we envisage that the photooxidation of  $\text{Fe}(\text{CO})_5$  in an  $\text{O}_2$ -doped argon matrix proceeds in accordance with the mechanism presented in Scheme I. Such a mechanism accounts successfully for the following observations: (i) the first appearance of  $\text{CO}_2$  with the destruction of the intermediate B; (ii) the finding that the formation of E probably requires the intervention of a second molecule of  $\text{O}_2$ ; (iii) the observation that C and D are formed at the expense of B when the matrix is annealed to 35 K for 10 min. That B is transformed to C and D at 35 K implies the onset of thermal decomposition reactions involving the elimination of  $\text{CO}$  and  $\text{CO}_2$ , respectively. This behavior is reminiscent of the reports of earlier studies carried out by Ozin et al.,<sup>58</sup> which have been interpreted in terms of the formation of the molecule gold(II) peroxyformate (XXVII) on cocondensation of gold atoms with  $\text{CO}/\text{O}_2$  mixtures at 20 K; when the resulting matrix is annealed to 30–40 K, thermal decomposition gives rise to  $\text{CO}_2$ .



It is interesting to compare the mechanism for the photooxidation of  $\text{Fe}(\text{CO})_5$  with that believed to govern the photooxidation of the group 6 hexacarbonyl molecules,  $\text{M}(\text{CO})_6$  ( $\text{M} = \text{Cr}, \text{Mo}, \text{or } \text{W}$ ), under similar conditions.<sup>10–13</sup> Some obvious similarities catch the eye. For example, intermediates A and B are plainly akin to the species  $(\eta^2\text{-O}_2)\text{M}(\text{CO})_4$  (VI) and  $\text{O}_2\text{M}(\text{CO})_2$  (VII), respectively, formed by the group 6 metals M. At the same time, there are several striking differences, as summarized below.

(i) The lack of photoselectivity in the  $\text{Fe}(\text{CO})_5/\text{O}_2$  system contrasts with the relatively high degree of photoselectivity which characterizes the  $\text{M}(\text{CO})_6/\text{O}_2$  systems ( $\text{M} = \text{Cr}, \text{Mo}, \text{or } \text{W}$ ) and which played an important part in their elucidation.<sup>11–13</sup>

(ii) The first detectable stage in the photooxidation of  $\text{Fe}(\text{CO})_5$  entails the uptake of an  $\text{O}_2$  molecule by the unsaturated photoproduct  $\text{Fe}(\text{CO})_4$ .<sup>20</sup> Oxidation of  $\text{M}(\text{CO})_6$  ( $\text{M} = \text{Cr}, \text{Mo}, \text{or } \text{W}$ ) appears, however, to require the loss of not one but two molecules of  $\text{CO}$  to form  $\text{M}(\text{CO})_4$  before  $\text{O}_2$  adds to the metal center; there is no sign of a product  $(\text{O}_2)\text{M}(\text{CO})_5$  derived from the addition of  $\text{O}_2$  to  $\text{M}(\text{CO})_5$ , the primary photoproduct of  $\text{M}(\text{CO})_6$ .<sup>29,59</sup> It

(57) Bajdor, K.; Nakamoto, K. *J. Am. Chem. Soc.* **1984**, *106*, 3045. Mizutani, Y.; Hashimoto, S.; Tatsuno, Y.; Kitagawa, T. *J. Am. Chem. Soc.* **1990**, *112*, 6809. Oertling, W. A.; Kean, R. T.; Wever, R.; Babcock, G. T. *Inorg. Chem.* **1990**, *29*, 2633. Proniewicz, L. M.; Paeng, I. R.; Nakamoto, K. *J. Am. Chem. Soc.* **1991**, *113*, 3294.

(58) Huber, H.; McIntosh, D.; Ozin, G. A. *Inorg. Chem.* **1977**, *16*, 975.

(59) Turner, J. J.; Burdett, J. K.; Perutz, R. N.; Poliakoff, M. *Pure Appl. Chem.* **1977**, *49*, 271.

is possible that this difference stems from the fact that  $\text{Fe}(\text{CO})_4$  has a triplet ground state, whereas each of the  $\text{M}(\text{CO})_5$  molecules of the group 6 metals M almost certainly has a singlet ground state.<sup>21</sup> Attention has already been drawn to the parallel between  $\text{Fe}(\text{CO})_4$  and an organic carbene (see section 1).<sup>23</sup> Intriguingly, however, experiments aimed at trying to detect a superoxoiron carbonyl derivative resembling the organic carbonyl oxide X, and formed by the thermal reaction between  $\text{Fe}(\text{CO})_4$  and  $\text{O}_2$ , were to no avail. On the other hand, the first detectable photoproduct A is plainly analogous to the organic dioxirane XI.

(iii) There is no sign of any molecule containing a linear dioxoiron moiety resembling  $\text{trans-O}_2\text{M}(\text{CO})_4$  (M = Mo or W).<sup>11</sup> This observation is not totally unexpected, since  $\text{trans-O}_2\text{Cr}(\text{CO})_4$  plays, at best, a minor role in the matrix photooxidation of  $\text{Cr}(\text{CO})_6$ . With  $\text{Ru}(\text{CO})_5$  or  $\text{Os}(\text{CO})_5$  as the precursor, the picture may be significantly different.

(iv) The first appearance of  $\text{CO}_2$  on UV photolysis of the  $\text{Fe}(\text{CO})_5/\text{O}_2$  system seems to be linked to the fate of the intermediate B and its photodissociation to form D, which we believe to be  $\text{OCFeO}$ . No intermediate analogous to D is observed during the photooxidation of a group 6 hexacarbonyl; indeed, the evolution of  $\text{CO}_2$  is not obviously linked to any one stage of the reaction sequence.<sup>11-13</sup>

(v) The  $\text{Fe}(\text{CO})_5/\text{O}_2$  system features an intermediate E which appears to require a second molecule of  $\text{O}_2$  for its formation. By contrast, the  $\text{M}(\text{CO})_6/\text{O}_2$  systems (M = Cr, Mo, or W) give rise

to no oxometal carbonyl intermediates of this type, and there is no suggestion that a second molecule of  $\text{O}_2$  becomes involved until the ultimate stages of the oxidation process are reached, with the formation of binary oxides of the type  $\text{MO}_3$  (M = Mo or W) or  $\text{WO}_4$  (XXVI).<sup>12,13,18</sup>

With these differences in mind, we will next turn our attention to the binary iron oxide molecules which are produced on prolonged photolysis of  $\text{O}_2$ -doped argon matrices containing  $\text{Fe}(\text{CO})_5$ .<sup>34</sup> The overall mechanism of the changes will then be reviewed in more detail.

**Acknowledgments.** We are grateful for support (i) from the SERC for the purchase of equipment and for funding a research assistantship (for M.J.A.) and a studentship (for M.F.) and (ii) from the Northern Ireland Department of Education for funding a studentship (for T.M.G.). We acknowledge with thanks the contributions of Professors M. Poliakoff and J. J. Turner through the computer programs which they kindly made available and through numerous helpful discussions. Studies of the  $\text{Fe}(\text{CO})_5/\text{O}_2$  system under matrix conditions were in fact initiated by this group,<sup>60</sup> including numerous experiments with pure  $\text{O}_2$  matrices but none involving isotopic enrichment of either the  $\text{Fe}(\text{CO})_5$  or the  $\text{O}_2$ ; the experimental results were in line with the ones described here.

(60) Smith, K. P. Ph.D. Thesis, University of Newcastle upon Tyne, 1981.

Contribution from the Inorganic Chemistry Laboratory, University of Oxford, Oxford OX1 3QR, U.K., and Department of Chemistry, University of Reading, Reading RG6 2AD, U.K.

## Photooxidation of Matrix-Isolated Iron Pentacarbonyl. 2. Binary Iron Oxide Reaction Products and the Overall Reaction Mechanism

Michael Fanfarillo,<sup>1a,b</sup> Anthony J. Downs,<sup>\*1a</sup> Tim M. Greene,<sup>1a</sup> and Matthew J. Almond<sup>1c</sup>

Received November 27, 1991

Binary iron oxide molecules F and G are generated, together with CO and  $\text{CO}_2$ , by prolonged UV photolysis ( $\lambda = \text{ca. } 312 \text{ nm}$ ) of  $\text{Fe}(\text{CO})_5$  molecules isolated in  $\text{O}_2$ -doped argon matrices at ca. 20 K. The identity and likely structure of each of the oxides have been established by analyzing the number, energies, and relative intensities of the IR absorptions displayed by the  $^{18}\text{O}$ -enriched molecule in the region  $800\text{--}1000 \text{ cm}^{-1}$ . Hence F is found to be the peroxide  $(\eta^2\text{-O}_2)\text{Fe}$ , in keeping with the conclusions drawn from earlier matrix experiments exploring the interaction of iron atoms with atomic and molecular oxygen. On the other hand, there seems little doubt that the ultimate product G is not  $\text{O}=\text{Fe}=\text{O}$ , as suggested previously, but the trioxide  $\text{FeO}_3$  with equivalent O atoms and a planar, or near-planar, skeleton conforming to  $D_{3h}$  symmetry. This represents the first positive identification of a binary iron(VI) compound. Taken together with the results presented in part 1, the findings point to a more-or-less complete reaction scheme for the matrix photooxidation of  $\text{Fe}(\text{CO})_5$ , as well as inviting comparisons with the details of related oxidation processes.

### 1. Introduction

In an earlier paper,<sup>2</sup> we presented the background to our investigations of the oxidation reactions induced by the UV photolysis of iron pentacarbonyl in an  $\text{O}_2$ -doped inert matrix at low temperatures. The IR spectrum of such a matrix witnesses the conversion of the parent carbonyl sequentially (albeit via more than one route) to the oxoiron carbonyl intermediates A–E, with the release of CO and  $\text{CO}_2$ , ultimately to arrive at two binary iron oxide molecules, F and G. The stoichiometry and likely structure of each of the intermediates A–E we were able to deduce, with varying degrees of confidence, by analysis of the number, energies, and intensity patterns of the IR absorptions associated with the  $\nu(\text{C}=\text{O})$  and  $\nu(\text{O}=\text{O})$  or  $\nu(\text{Fe}=\text{O})$  fundamentals. Here we turn our attention to the final stages of the photooxidation of ma-

trix-isolated iron pentacarbonyl, whereat none of the CO remains coordinated to the metal. We concentrate on the characterization of the products F and G, with the aim of gaining a fuller understanding of the whole reaction scheme set in train by UV irradiation of  $\text{Fe}(\text{CO})_5/\text{O}_2$  mixtures supported in a matrix environment.

### 2. Experimental Section

The experiments were carried out using the low-temperature apparatus and procedures described elsewhere.<sup>2-6</sup> Matrices were usually prepared by pulsed deposition.<sup>7</sup> IR spectra were recorded with a Perkin-Elmer Model 580A dispersive spectrophotometer affording a resolution and accuracy not exceeding  $0.5 \text{ cm}^{-1}$ ; there was no provision for carrying out

(1) (a) University of Oxford. (b) Present address: Pharmaceutical Department, ICI Pharmaceutical Division, Hurdsfield Industrial Estate, Macclesfield, Cheshire, SK10 2NA, U.K. (c) University of Reading.  
(2) Fanfarillo, M.; Cribb, H. E.; Downs, A. J.; Greene, T. M.; Almond, M. J. *Inorg. Chem.*, preceding paper in this issue.

(3) Almond, M. J.; Crayston, J. A.; Downs, A. J.; Poliakoff, M.; Turner, J. J. *Inorg. Chem.* **1986**, 25, 19.

(4) Crayston, J. A.; Almond, M. J.; Downs, A. J.; Poliakoff, M.; Turner, J. J. *Inorg. Chem.* **1984**, 23, 3051.

(5) Almond, M. J.; Downs, A. J. *J. Chem. Soc., Dalton Trans.* **1988**, 809.

(6) Almond, M. J.; Hahne, M. J. *J. Chem. Soc., Dalton Trans.* **1988**, 2255.

(7) Perutz, R. N.; Turner, J. J. *J. Chem. Soc., Faraday Trans. 2* **1973**, 69, 452.